NEUROSCIENCE

Synaptic targets of circadian clock neurons influence core clock parameters

Eva Scholz-Carlson[1,2], Aishwarya R. Iyer[1], Aljoscha Nern[3], John Ewer[4,5], Maria P. Fernandez[1,2]*

Neuronal connectivity in the circadian clock network is essential for robust endogenous timekeeping. In the *Drosophila* circadian clock network, the small ventral lateral neurons (sLN$_v$s) serve as critical pacemakers. Peptidergic communication mediated by the neuropeptide *Pigment Dispersing Factor* (PDF), released by sLN$_v$s, has been well characterized. In contrast, little is known about the role of the synaptic connections that sLN$_v$s form with downstream neurons. Connectomic analyses revealed that the sLN$_v$s form strong synaptic connections with previously uncharacterized neurons called superior lateral protocerebrum 316 (SLP316). Here, we show that silencing the synaptic output from the SLP316 neurons via tetanus toxin expression shortened the free-running period, whereas hyperexciting them by expressing the bacterial voltage-gated sodium channel resulted in period lengthening. Under light-dark cycles, silencing SLP316 neurons caused lower daytime activity and higher daytime sleep. Our results reveal that the main postsynaptic partners of key *Drosophila* pacemaker neurons are a nonclock neuronal cell type that regulates the timing of sleep and activity.

INTRODUCTION

Circadian rhythms, which allow animals to anticipate day-night changes in their environment, are generated by small groups of neurons in the brain that contain molecular clocks (*1*). These neurons form a network with synchronized molecular oscillations (*2*, *3*). The maintenance of robust and coherent behavioral circadian rhythms depends on connectivity within the clock network, which controls the timing of key behavioral outputs such as rhythms in feeding, mating, and sleep (*3*). In both mammals and flies, connectivity within the clock network is mediated by peptide and transmitter outputs (*4*–*7*). Although the molecular mechanisms driving endogenous oscillations in clock neurons are well described, the pathways through which these neurons communicate with each other and with downstream targets to propagate oscillations throughout the brain remain poorly understood.

Drosophila melanogaster is an ideal model for studying connectivity in the clock network. The fly circadian network consists of ~240 neurons [(*8*), reviewed in (*9*)] and is the functional equivalent of the mammalian suprachiasmatic nuclei (SCNs), the principal clock in the vertebrate brain (*10*, *11*). Each clock neuron within this network has an intracellular molecular timekeeping mechanism based on a transcriptional-translational feedback loop (*12*). Clock neurons can be organized into seven main groups based on their anatomical location (*11*, *13*–*16*). Whereas the molecular oscillations of most of these groups are in phase, some major clock groups become active at specific times of day, which correlates with their roles in controlling behavioral outputs (*17*). Among these cells, the small ventral lateral neurons (sLN$_v$s) are key for maintaining rhythmicity under conditions of constant darkness (DD) and temperature and are considered the dominant circadian pacemakers under these conditions (*18*–*21*). Despite the importance of these cells for sustaining physiological and behavioral rhythms, very little is known about their connectivity with target neurons. An analysis of their synaptic connectivity revealed that they form very few monosynaptic connections with other clock neurons (*16*).

Peptidergic signaling is essential for clock network intercommunication and output (*6*). The neuropeptide *Pigment Dispersing Factor* (PDF), which is secreted by the sLN$_v$s, is required for synchronizing molecular oscillations within the network, setting the phase of neural activity in other groups of clock neurons, and maintaining activity-rest rhythms under constant conditions (*18*, *22*–*24*). Expression of PDF undergoes daily and circadian oscillations in the dorsal terminals of the sLN$_v$ (*19*), and the loss of PDF or the PDF receptor (PDFR) results in arrhythmicity under free-running conditions (*25*–*27*). In addition to PDF, the sLN$_v$s express the neuropeptide short neuropeptide F (sNPF) (*28*), which promotes sleep and is involved in feeding regulation (*28*–*30*) and eclosion rhythms (*31*), and the inhibitory neurotransmitter glycine (*32*). Down-regulation of *bruchpilot* (*brp*) and other synaptic active zone proteins expressed by the sLN$_v$s does not affect rhythmicity, and dense-core vesicle release profiles of the sLN$_v$s in the Full Adult Fly Brain (FAFB) do not show spatial overlap with BRP-labeled active zones (*33*). This finding is consistent with the observation that neuropeptide release takes place from sites located all along the sLN$_v$, including the soma (*34*), and with the persistence of robust behavioral rhythmicity upon silencing of synaptic transmission (*35*) in *Pdf*$^+$ neurons (*36*, *37*).

Although the circadian clock provides predictability, it must also be flexible to adapt to varying environmental conditions. Distinct subsets of neurons control the morning and evening bouts of activity that produce the bimodal pattern that flies show under light-dark (LD) cycles. The sLN$_v$s, which are active around dawn (*17*), are associated with the morning peak of activity (*18*, *20*, *21*) and are called morning (M) cells. The PDFR-expressing dorsal lateral neurons and the PDF-negative fifth LN$_v$ are associated with the evening activity peak (*20*, *21*, *38*), and their neural activity is maximal before dusk (*17*). Some dorsal neurons (DNs) also contribute to the timing and amount of activity and sleep via the modulation of M and E (evening) cells (*39*–*42*). The control of the M and E bouts of activity by different neurons allows the fly's pattern of activity to adjust to the changes in environmental conditions of light and temperature experienced during the different seasons (*43*–*48*).

[1]Department of Biology, Indiana University Bloomington, Bloomington, 47401 IN, USA. [2]Department of Neuroscience and Behavior, Barnard College, New York City, 10027 NY, USA. [3]Janelia Research Campus, Howard Hughes Medical Institute, Ashburn, 20147 VA, USA. [4]Instituto de Neurociencia, Universidad de Valparaíso, Valparaíso 2360102, Chile. [5]Centro Interdisciplinario de Neurociencias de Valparaíso, Universidad de Valparaíso, Valparaíso 2360102, Chile.
*Corresponding author. Email: fernanm@iu.edu

The four sLN$_v$s form few direct synaptic connections with other clock neurons or other neurons outside the clock network, yet they form strong connections with a previously uncharacterized group of neurons named superior lateral protocerebrum 316 (SLP316). The SLP316 cells synapse onto the DN1pA class of dorsal clock neurons, which are associated with the reorganization of sleep/wake cycles [reviewed in (*41*)]. Here, we show that despite not being clock neurons themselves, silencing SLP316 neuronal activity resulted in a small but robust shortening of the free-running period of activity, whereas their excitation resulted in the opposite phenotype. Neither manipulation led to the loss of rhythmicity. Under LD cycles, manipulations of the SLP316 activity led to a reduction in evening activity and an increase in sleep, both under an ambient temperature of 25°C and under cold, winter-like days. Under both LD and DD, the behavioral phenotypes observed were different from those caused by the loss of PDF. In conclusion, our data reveal a role in regulating the timing of sleep/wake cycles of a previously unknown neuronal population that connects two classes of clock neurons but is not itself part of the circadian clock network.

RESULTS

Connectomic datasets identify SLP316 neurons as primary postsynaptic partners of sLN$_v$s

On the basis of the *Drosophila* hemibrain connectome (*49*), the sLN$_v$s form much stronger connections with an uncharacterized neuronal cell type than with any other neurons, including other clock neurons (Fig. 1A) (*16*). This cell type, called SLP316, consists of three neurons with somas in the dorsal-most region of the SLP (*49*). The sLN$_v$s are, in turn, the main presynaptic inputs to SLP316 neurons (Fig. 1, A and B). Most inputs to SLP316 cells from their top 10 presynaptic partners are located along the ventromedial projections, whereas their output synapses are concentrated along the dorsal arborizations (Fig. 1C).

The synapses formed by the sLN$_v$s onto the SLP316 neurons represent 70% of the synapses by all groups that form strong connections with these cells (weight > 10) (Fig. 1, A and B). Many of the synapses that the sLN$_v$s form onto the SLP316s (~20%) are located below the point at which the sLN$_v$s extend and ramify their dorsal termini (fig. S1A), the region long thought to be the location of sLN$_v$ output synapses. The

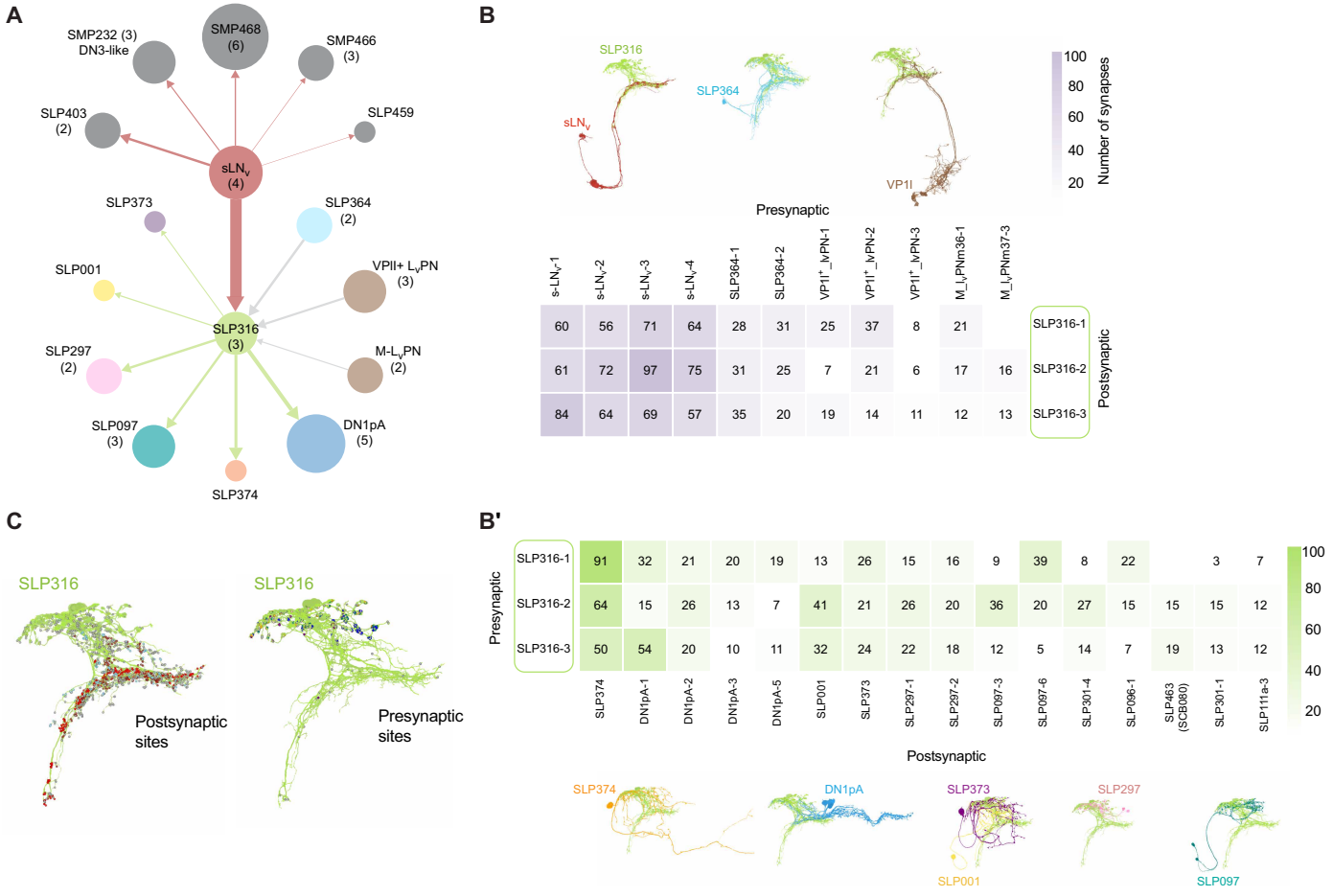

Fig. 1. SLP316 neurons are the main postsynaptic partner of the sLN$_v$s. (**A** and **B**) Connectomic mapping from the hemibrain dataset. (A) Map of top input/output neuronal groups to/from the SLP316s and from the sLN$_v$s. The number of neurons in each group is indicated in parentheses if greater than one and reflected by circle size. Connection strength between cell types is represented by arrow width and decreases in a clockwise direction for each connection type (input/output). SLP232 likely corresponds to DN3s. (B) Strong shared inputs to and (B′) outputs of the SLP316s (>10 synapses to/from at least two SLP316 neurons) with neuronal morphology shown above or below. (**C**) Input synapses to and output synapses of the three SLP316 neurons (SLP316_R_1, SLP316_R_2, and SLP316_R_3) shown in green, excluding synapses from neuron segments. Synapse color corresponds to neuron color in (A) and (B), and all other synapses are shown in gray.

other main inputs to SLP316 are from two neurons that belong to the SLP364 cell type and from ventroposterior (VP) antennal lobe glomerulus neurons. The SLP316s are innervated largely by neurons not only in the SLP neuropil but also from the superior medial (SMP) and posterior lateral (PLP) protocerebrum (fig. S1B).

The SLP316 neurons are largely homogeneous in their connectivity patterns with upstream neurons, but their outputs are more varied (Fig. 1B); they form some of the strongest connections with another group of clock neurons, the posterior DNs (DN1p). The DN1pA class of clock neurons is the top output of the SLP316 cells. The main neuropil innervated by SLP316s is the SLP, followed by the SMP and PLP with a much smaller number of connections (fig. S1B). We next examined the connectivity patterns of the sLN_vs in the FlyWire *Drosophila* connectome (*50*) to determine whether cells with similar morphology to that of the SLP316s were among their top postsynaptic partners. We found that in both hemispheres, the sLN_vs formed most of their output synapses with cells that were highly similar in location and morphology to SLP316s (fig. S1, C and D). Computational predictions based on synapse architecture for both the hemibrain and FAFB-Flywire datasets (*51*) indicated that SLP316 cells are likely glutamatergic (fig. S1E). A list of the FAFB neuron IDs is included in table S2.

The SLP316 neurons are nonclock neurons that extend along the sLN_v projection tract

To further study the SLP316 neurons, we generated a *split-GAL4* line that targeted these cells (#SS76489; see Materials and Methods) (fig. S2A). Because both the hemibrain and FAFB/FlyWire connectomes correspond to an adult female (*49*), we dissected brains from both *SLP316 > mCD8-GFP* males and females to determine whether there were sex differences in the number of cells or their morphology. The projections from the SLP316 neurons extended toward the ventral brain along the same tract as the projections of the sLN_vs, which extend from the ventral to the dorsal brain (Fig. 2, A to D). The number of labeled SLP316 cells decreased from 1-day-old flies to 1-week-old flies (Fig. 2E and fig. S2B), and we did not observe sex differences at either stage (Fig. 2E). The number of labeled cells remained similar in older flies (5 weeks old; fig. S2C). In 1-week-old flies, we did not detect any specific expression in the ventral nerve cord (fig. S2D). Therefore, we conclude that the driver is likely specifically expressed in SLP316 neurons in adults and that the expression pattern is similar in males and females.

The SLP316 neurons are in the dorsoposterior area of the brain, where the DN1ps are located. To determine whether these cells were yet unidentified clock neurons, we costained with a PER antibody. Adult *SLP316 > mCD8-GFP* flies were entrained to a 12-hour:12-hour LD cycle for 5 days, and brains were dissected at the end of the night Zeitgeber time 23 (ZT23), when PER nuclear signal is strongest (*52*). We did not detect PER nuclear signal in the somas of any of the SLP316 cells (Fig. 2, F to H). Therefore, we conclude that the SLP316 neurons are not circadian clock neurons. To determine whether there were daily changes in excitability in these cells, we used a transcriptional reporter in which the *Hr38* regulatory DNA is upstream of a nuclear-localized fluorescent Tomato reporter (*53*). In the sLN_vs, the *Hr38-Tomato* reporter gene showed higher expression around ZT2, as reported by a previous study (*54*). In contrast, SLP316 cells consistently showed a low signal (fig. S2, E and F). Because of the low intensity of the red fluorescent protein (RFP) signal in these cells, the presence of physiological rhythms cannot be excluded.

Next, we assessed connectivity between the cells labeled by the SLP316 *split-GAL4* line and the sLN_vs via BAcTrace. This is a retrograde synaptic tracing technique in which *Clostridium botulinum* neurotoxin A1 (BoNT/A) is transferred from a postsynaptic donor cell (driven by Gal4 components) to a presynaptic receiver cell (driven by LexA components) by targeting the interior of a synaptic vesicle (*55*). In the receiver cell, the toxin releases a membrane-localized transcription factor, inducing Tomato expression. When a vesicle is recycled, the toxin is internalized into the cell, thereby labeling the presynaptic neuron. We combined flies expressing the BAcTrace transgenes (see Materials and Methods) with flies carrying both the SLP316 *split-GAL4* and the *Pdf-LexA* transgenes and stained brains with antibodies against PDF, RFP, and green fluorescent protein (GFP) (Fig. 2, I to M). Experimental flies showed RFP signal in the sLN_vs, but not the lLN_vs (large ventral lateral neurons), whereas PDF immunoreactivity was detected in both groups of LN_vs (Fig. 2, I, K, and L). Control flies without the SLP316 *split-GAL4* driver did not express RFP (Fig. 2G). As expected, GFP signal could be detected in both the sLN_vs and lLN_vs (Fig. 2, M and P). We did not observe sex differences in the expression pattern in experimental or control flies. These results support the notion that the SLP316 neurons are postsynaptic partners of the sLN_vs, which is consistent with connectomic data.

Altering the activity of SLP316 neurons changed the free-running period

Elimination of the LN_vs via expression of the proapoptotic gene *hid* leads to severe loss of rhythmicity and shortening of the free-running period, similar to the behavioral phenotypes caused by the *Pdf* null mutation, Pdf^{01} (*18*). In addition, whereas inhibiting synaptic transmission from *Pdf* neurons via tetanus toxin (TNT) does not affect the ability of the flies to maintain rhythmicity in DD, it leads to changes in free-running period, as *Pdf > TNT* flies show longer periods than do their parental controls (*36*, *37*, *56*). Because the SLP316s are the main cell type downstream of the clock pacemaker neurons, we asked how manipulating these cells would affect behavioral rhythms.

The bacterial voltage-gated sodium channel (*NaChBac*) is used to increase neuronal excitability [reviewed in (*57*)]. Expression of *NaChBac* in *Pdf*-expressing neurons results in complex rhythms, with multiple superimposed period components under free-running conditions (*58*). In contrast, expressing *NaChBac* in the SLP316 cells caused a small but significant lengthening of the free-running period without affecting overall rhythmicity (Fig. 3, A to C, and Table 1), similar to the phenotype observed upon silencing activity of the Pdf^+ neurons via TNT. After 8 days in DD, experimental flies showed a 3.3-hour phase delay in their activity peak (Fig. 3, D and E). Under an LD cycle, *SLP316 > NaChBac* flies showed a significant reduction in daytime activity (fig. S3, A and B). However, the timing of the morning and evening activity peaks was not affected (fig. S3, C to E).

Next, we expressed *hid* under the SLP316 driver. Under DD, *SLP316 > hid* flies showed small but robust changes in free-running period (Fig. 3, F and G). The overall number of rhythmic flies and the power of their rhythm were not affected (Fig. 3H and Table 1). A phase advance in activity could be detected on day 8 under DD conditions (fig. S3, P and Q). *SLP316 > hid* females also showed a shortening in free-running period and no effect on the overall number of rhythmic flies (fig. S4, A, B, and E). Therefore, targeted death of most SLP316 cells and *NaChBac*-mediated hyperexcitation

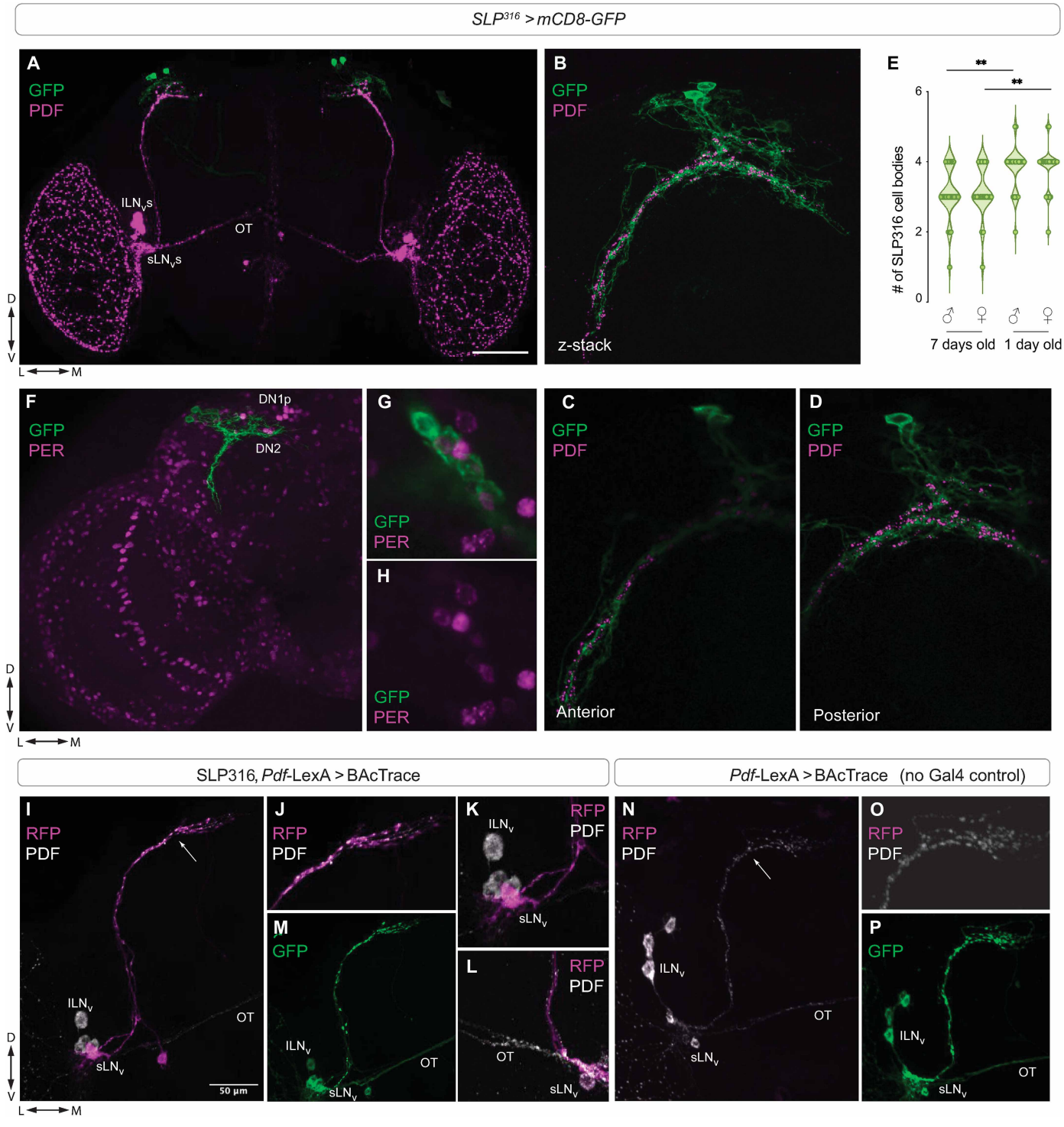

Fig. 2. The SLP316 driver labeled nonclock neurons that share functional synapses with the sLN$_v$s. (**A** to **D**) Representative confocal images of a brain from a 7-day-old *SLP316 > GFP* male fly stained with antibodies against green fluorescent protein (GFP; green) and PDF (magenta). (A) Whole brain, (B) SLP z-stack, and anterior (C) and posterior (D) single optical slices (step size of 0.9 µm). D, dorsal; V, ventral; L, lateral; M, medial. (**E**) Quantification of cell body count on the left hemisphere labeled by the *SLP316* driver in 7- and 1-day-old male and female flies from three replicate experiments ($n > 21$ for each group). (**F** to **H**) Representative confocal images of a brain hemisphere of a 6- to 7-day-old *SLP316 > GFP* male brain stained with antibodies against GFP (green) and PERIOD (PER) (magenta). (**I** to **M**) Representative confocal images of *SLP316-Gal4* and *Pdf-LexA* driving expression of BAcTrace components. Red fluorescent protein (RFP) signal can only be detected in the sLN$_v$s. (J) sLN$_v$ dorsal termini show PDF and RFP expression. (K) Cell bodies of sLN$_v$s and lLN$_v$s. (L) sLN$_v$ cell bodies plus dorsal projections show RFP signal, whereas the lLN$_v$s do not. (M) Synaptobrevin (syb)-GFP expression in the small and large LN$_v$s in experimental brains. (**N** to **P**) Representative confocal images of *Pdf-LexA* driving expression of BAcTrace components without the SLP316-Gal4 driver. (P) syb-GFP expression in the small and large LN$_v$s in control brains. Scale bars, 50 µm (all). OT, Optic Tract. *$P < 0.05$, **$P < 0.01$, ***$P < 0.001$.

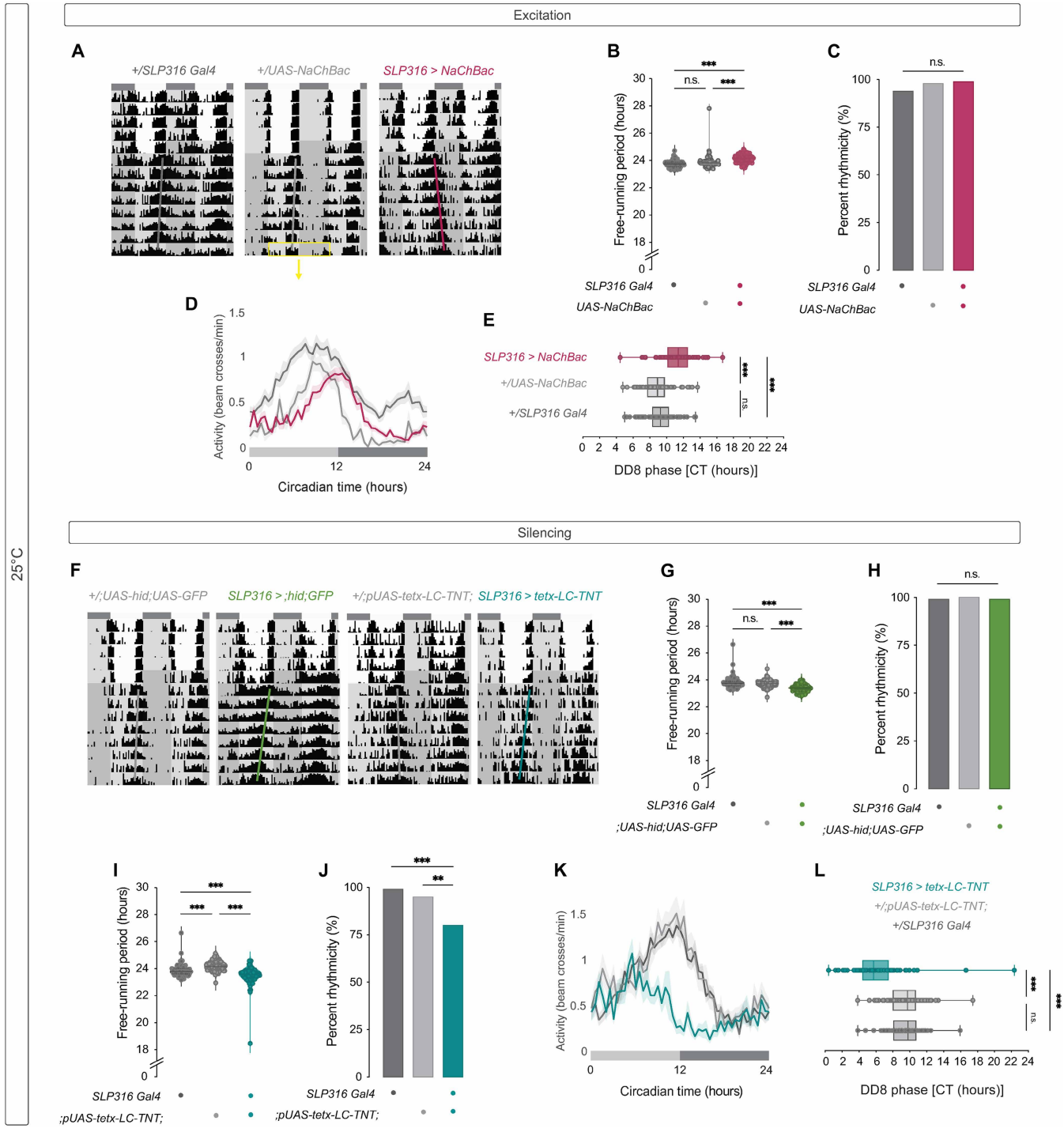

Fig. 3. Manipulation of the SLP316s altered free-running period length. (**A**) Representative double-plotted actograms, (**B**) free-running period calculated using the chi-square periodogram, and (**C**) percentage of rhythmic flies for control (*SLP316 split-GAL4* and *UAS-NaChBac*) and experimental (*SLP316 > NaChBac*) flies. n.s., not significant. (**D**) Activity plot on the eighth day of free running, indicated in (A) with a yellow box. (**E**) Phase of activity from (D), calculated in ClockLab using a sine fit of the waveform of activity. CT, circadian time. (**F**) Representative actograms, (**G**) free-running period, and (**H**) percentage of rhythmic flies for control (*w;UAS-hid;UAS-GFP* and *w;pUAS-tetx-LC-TNT;*) and experimental (*SLP316 > hid + GFP* or *SLP316 > tetx-LC-TNT*) flies. (**I**) Free-running period, and (**J**) percentage of rhythmic flies for control (*SLP316 split-GAL4* and *;pUAS-tetx-LC-TNT;*) and experimental *(SLP316 > tetx-LC-TNT*) flies. (**K**) Activity plot and (**L**) phase of activity on the eighth day of free running for control (*SLP316 split-GAL4* and *;pUAS-tetx-LC-TNT;*) and experimental *(SLP316 > tetx-LC-TNT*) flies. Actograms show 5 days of LD, followed by 9 days of DD. Flies were raised, and activity-rest behavior was recorded at 25°C. Rhythmic power was calculated using the chi-square periodogram in ClockLab using 30-min activity bins, and flies with a rhythmic power of 10 or greater were classified as rhythmic. Free-running period was calculated for rhythmic flies using the chi-square periodogram routine of ClockLab using 1-min activity bins. Statistical comparisons were conducted using the Kruskal-Wallis test, followed by Dunn's multiple comparisons test for free-running period and phase of activity, and using Fisher's exact test for the number of rhythmic and arrhythmic flies. Data from three replicate experiments are plotted for each genotype. *$P < 0.05$, **$P < 0.01$, ***$P < 0.001$.

Table 1. Summary of free-running activity rhythm parameters. Activity analysis of the indicated genotypes, at either 25° or 18°C. Light conditions for each experiment were a 12-hour:12-hour LD-DD cycle. For each genotype, the number of flies (*n*) is listed above. All flies were raised at 25°C. ClockLab's chi-square periodogram analysis was used to analyze rhythmicity, rhythmic power, and free-running period for each genotype. The percent rhythmicity, along with the number of rhythmic flies (*n*R), the period in hours with the SEM, and the power of the rhythmicity with the SEM are indicated. Arrhythmic flies were not considered in the analysis. M, male; F, female.

Temperature: 25°C					
Genotype	**Sex**	**Number of flies (*n*)**	**% Rhythmicity (*n*R)**	**Period (hours) ± SEM**	**Rhythmic power ± SEM**
;Pdf-Red,Pdf-Gal4;	M	90	100 (90)	24.57 ± 0.04	148.3 ± 6.06
;pUAS-tetx-LC-TNT;	M	113	96.46 (109)	24.11 ± 0.04	91.38 ± 4.75
;Pdf-Red,Pdf-Gal4; > ;tetx-LC-TNT;	M	76	78.95 (60)	24.99 ± 0.11	64.58 ± 5.45
SLP316 split-GAL4	M	170	95.88 (163)	23.82 ± 0.03	117.4 ± 4.14
NaChBac	M	73	98.63 (72)	23.91 ± 0.06	172.0 ± 5.82
SLP316 > NaChBac	M	69	98.55 (68)	24.13 ± 0.04	171.0 ± 5.30
;UAS-hid;UAS-GFP	M	76	100 (76)	23.73 ± 0.03	167.9 ± 5.39
SLP316 > ;hid;GFP	M	68	98.80 (82)	23.38 ± 0.04	144.5 ± 6.98
SLP316 > ;tetx-LC-TNT;	M	85	80.0 (68)	23.47 ± 0.09	41.02 ± 3.46
SLP316 split-GAL4	F	31	80.65 (25)	24.41 ± 0.12	89.78 ± 11.06
;UAS-hid;UAS-GFP	F	32	100 (32)	24.39 ± 0.06	174.5 ± 8.34
SLP316 > ;hid;GFP	F	32	100 (32)	24.26 ± 0.26	169.1 ± 11.20
;pUAS-tetx-LC-TNT;	F	29	93.10 (27)	25.14 ± 0.34	117.4 ± 10.96
SLP316 > ;tetx-LC-TNT;	F	31	96.77 (30)	24.25 ± 0.07	131.1 ± 7.69
Temperature: 18°C					
Genotype	**Sex**	**Number of flies (*n*)**	**% Rhythmicity (*n*R)**	**Period (hours) ± SEM**	**Rhythmic power ± SEM**
SLP316 split-GAL4	M	160	97.50 (156)	23.86 ± 0.11	81.45 ± 2.87
NaChBac	M	32	100 (32)	23.72 ± 0.06	100.7 ± 5.74
SLP316 > NaChBac	M	32	100 (32)	23.70 ± 0.07	106.5 ± 6.93
;UAS-hid;UAS-GFP	M	94	100 (94)	23.78 ± 0.03	121.5 ± 4.91
SLP316 > ;hid;GFP	M	92	89.13 (82)	23.53 ± 0.18	67.05 ± 4.41
;pUAS-tetx-LC-TNT;	M	94	79.79 (75)	23.83 ± 0.18	49.49 ± 3.57
SLP316 > ;tetx-LC-TNT;	M	95	68.42 (65)	23.45 ± 0.17	36.00 ± 2.84
*Pdf*01	M	31	93.55 (29)	23.88 ± 0.04	63.02 ± 6.584
SLP316 split-GAL4	F	63	84.13 (53)	24.12 ± 0.18	79.16 ± 6.03
;UAS-hid;UAS-GFP	F	25	84.00(21)	24.15 ± 0.13	66.93 ± 7.93
SLP316 > ;hid;GFP	F	26	92.31 (24)	23.54 ± 0.56	84.16 ± 9.95
;pUAS-tetx-LC-TNT;	F	64	93.75 (60)	24.29 ± 0.06	103.9 ± 6.31
SLP316 > ;tetx-LC-TNT;	F	58	91.38 (53)	23.75 ± 0.09	82.40 ± 5.64

of these cells led to opposite phenotypes in the free-running period of activity rhythms.

To determine whether synaptic activity was responsible for the effects on periodicity, we expressed TNT (*35*) in the SLP316 neurons. This manipulation also resulted in a shortening of the free-running period (Fig. 3, F and I, and Table 1). We also observed a small reduction in the percentage of rhythmic flies and a phase advance on DD8 of ~3.2 hours (Fig. 3, J to L). In *SLP316 > TNT* females, the free-running period was not significantly different from that of controls (fig. S4, C to E). Under LD, both *hid* and *TNT* expressions in the SLP neurons resulted in a reduction in daytime activity in males (fig. S3, G and L). Shortening of the free-running period is typically associated with an early phase of the evening peak of activity under an LD cycle, such as occurs in Pdf^{01} mutants or in flies in which *Shaggy* or *Doubletime* (DBT^{S}) are expressed in the sLN_vs (*59*, *60*). However, the LD activity profiles of *SLP316 > hid* and *SLP316 > TNT* flies showed that these flies could anticipate the lights-on transition normally (fig. S3, F and K). Moreover, we did not observe a significant change in the phase of the morning or evening peaks of activity in either *SLP316 > hid* or *SLP316 > TNT* flies (fig. S3, H, I, M, and N). Nevertheless, the area under the evening peak was significantly lower in experimental flies than in the controls, indicating lower activity at this time of day (fig. S3, J and O). To determine whether adult-specific silencing of SLP316 cells leads to changes in behavioral rhythms, we expressed $Shibire^{ts}$, a temperature-sensitive mutation in dynamin, in these cells (*61*, *62*). Flies were raised at 19°C and transferred to 29°C upon eclosion, and experiments were conducted at 29°C. Control groups were

kept at 19°C throughout development, and experiments were conducted at 19°C. We observed a significant lengthening of the free-running period in experimental flies at high temperature (fig. S5A).

The only behavioral rhythm that is mediated by the LN_vs but does not rely on PDF is adult emergence from the pupal case (eclosion) (*31*, *63*). The larval LNs, which survive metamorphosis and become the adult sLN_vs (*64*), communicate with the Prothoracicotropic hormone (PTTH)-expressing neurons to regulate eclosion rhythms (*31*). In pharate adults, the sLN_vs inhibit PTTH neuron Ca^{2+} activity via sNPF, not PDF, and the PTTH neurons appear to be postsynaptic targets of the sLN_vs based on transsynaptic tracing experiments (*31*). In addition, PTTH neurons express sNPF and not PDFRs (*31*). To determine whether manipulations of SLP316 neurons affected eclosion rhythms, we conducted population experiments in which these cells were eliminated via expression of *hid*. We did not detect eclosion rhythm phenotypes in experimental *SLP316* > *hid* flies (Fig. 4, A and B). Similarly, expression of another proapoptotic gene, *reaper*, had no effect on eclosion rhythms (fig. S5, B and C). Together, these results show that manipulations of the SLP316 neurons affected free-running rhythms in activity, but not eclosion rhythms.

Organization of activity under cold days was disrupted upon SLP316 silencing

Because a subset of the DN1p class of clock neurons are major postsynaptic partners of the SLP316 cells, we investigated the effect of manipulating these cells under low-temperature 12-hour:12-hour LD cycles, where the DN1ps appear to play a more prominent role in shaping activity (*46*). Thus, for example, only under conditions of low light intensity, low temperature, or low or absent PDF, can rescuing the molecular clock in a subset of glutamatergic DN1ps promote an evening peak of activity (*45*, *46*).

Low temperatures lead to a reorganization of activity in wild-type flies, as they adapt to the shorter days of winter. Under low-temperature (18°C) LD cycles, the distance between the morning and evening peaks is reduced, primarily due to a substantially earlier phase of the evening peak, which decreases the phase angle of entrainment (*43*). We exposed flies in which we eliminated or silenced SLP316 cells to LD cycles under cold temperatures. *SLP316* > *hid* flies showed significantly reduced daytime activity and increased daytime sleep compared to controls (Fig. 5, A to D). Similar phenotypes, both in terms of daytime activity and daytime sleep, were observed in experimental *SLP316* > *TNT* (Fig. 5, E to H) and *SLP316* > *NaChBac* flies (fig. S6, K, L, N, and O). Neither nocturnal activity nor sleep was affected (fig. S6, A to D and M and P).

Under free-running conditions, manipulations of SLP316 neuron activity and the loss of *Pdf* result in different phenotypes. The Pdf^{01} mutant is predominantly arrhythmic (*18*). However, the Pdf^{01} flies that remain rhythmic exhibit a shortened free-running period, similar to the effect observed after silencing SLP316 neurons (*18*). However, under LD conditions, manipulations of SLP316 neurons did not cause the expression of the classic phenotypes associated with the loss of *Pdf*, such as a lack of morning anticipation or an advanced evening peak (fig. S3). The advanced evening peak is thought to result from a phase-delay effect of PDF on E cells: In the absence of PDF, neuronal activity in the E cells shows a large phase advance (*24*). PDF levels are temperature sensitive, increasing during hot, summer-like days, and decreasing under colder conditions (*65*).

We exposed Pdf^{01} flies to the same LD 18°C cycles and observed a significant advance in the evening peak and a 1.5-fold increase in daytime activity (Fig. 5, I and J). This indicates that the early peak observed in wild-type flies under LD (*43*) is not solely attributable to the reduction in PDF observed under lower temperatures because flies that lack PDF show a pronounced shift in evening activity. *Pdf* mutants show higher levels of daytime sleep in 12-hour:12-hour LD cycles at 25°C (*66*); however, the pronounced increase in evening activity under an LD 18°C cycle was accompanied by an overall decrease in daytime sleep (Fig. 5, K and L). The onset of activity was earlier, and activity levels remained high until the lights-off transition. After the lights-off transition, activity and sleep levels between control and Pdf^{01} flies became more similar (Fig. 5, I and K); nevertheless, there remained a small but significant increase in nocturnal activity but no differences in sleep (fig. S6, E and F).

Previous studies have shown that low temperatures (<18°C) can substantially advance the phase of the evening activity peak by ~3 hours (*65*, *67*). Consistent with this, both experimental and control lines exhibited an earlier evening phase at 18°C relative to that at 25°C (compare fig. S6, G and H, to fig. S3, I and N; table S1), but we found no differences between experimental and control flies at either temperature. To determine whether earlier evening activity may reveal

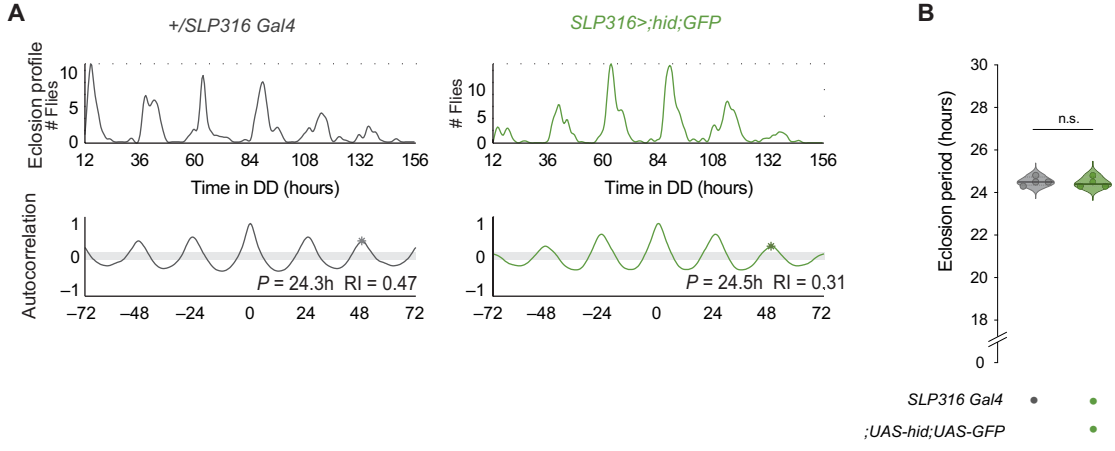

Fig. 4. Silencing or eliminating SLP316 neurons did not affect the eclosion rhythm. (**A**) Records showing the time course of emergence of flies under DD conditions (left), their corresponding autocorrelation analysis (middle), and periodicities (right). (**B**) Period of eclosion of populations of flies of the indicated genotypes.

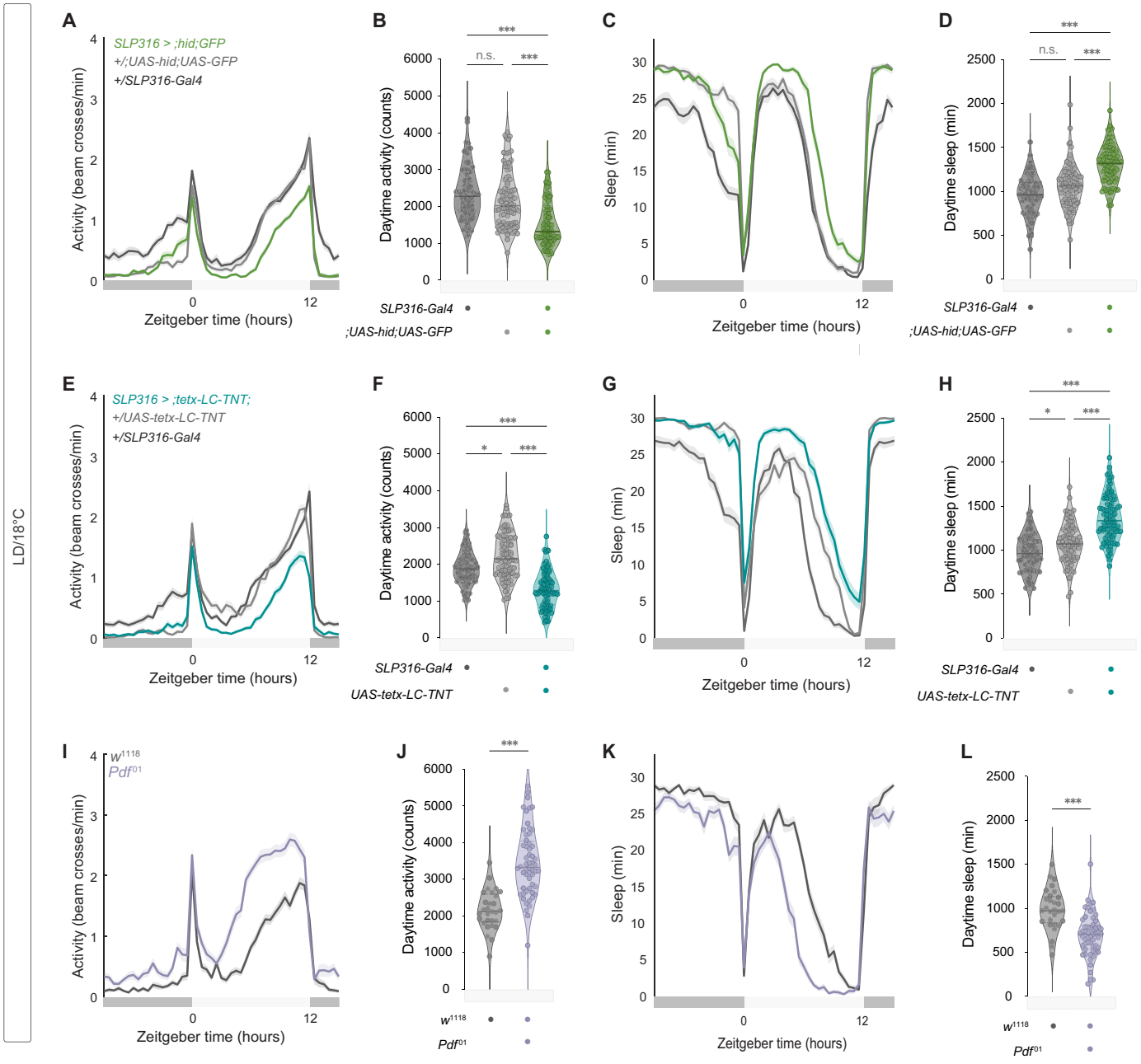

Fig. 5. *Pdf* and SLP316 disruption have opposite effects on daytime activity and sleep quantities under cold temperature. (**A** to **D**) Activity and sleep phenotypes of *SLP316 > hid + GFP* flies during 3 days of 12-hour:12-hour LD cycle at 18°C. Representative activity (A) and sleep (C) plots averaged for control (*SLP316 split-GAL4* and *w;UAS-hid;UAS-GFP*) and experimental (*SLP316 > hid + GFP*) flies. Daytime (ZT0 to ZT12) (B) activity counts and total sleep amount (D). (**E** to **H**) Activity and sleep phenotypes of *SLP316 > ;tetx-LC-TNT* flies and parental controls. Representative activity (E) and sleep (G) plots, and their respective quantifications (F and H). (**I** to **L**) Activity and sleep phenotypes for wild-type w^{1118} and pdf^{01} flies. Representative activity (I) and sleep (K) plots, and total daytime activity counts (J) and sleep amount (L). Flies were raised at 25°C, and activity-rest behavior was recorded at 18°C. Statistical comparisons were conducted using the Kruskal-Wallis test, followed by Dunn's multiple comparisons test for comparisons between three genotypes in (B), (D), and (F) and (H), and using the Mann-Whitney test for comparisons between two genotypes in (J) and (L). Data plotted are from two replicate experiments for (B), (D), and (F) and (H) and three replicate experiments for each genotype for (J) and (L). $*P < 0.05$, $**P < 0.01$, $***P < 0.001$

phase differences, we extended our analysis to LD cycles at 16° and 14°C. The results were consistent with those obtained at higher temperatures: *SLP316 > TNT* flies exhibited reduced daytime activity, while the phase of the evening peak of activity was not significantly different from that of controls (figs. S6, G to J, and S7, A to H). These findings indicate that under cold-day conditions, the loss of *Pdf* and the silencing or elimination of SLP316 neurons produce distinct behavioral phenotypes.

Silencing SLP316 neurons increased daytime sleep

Under standard LD conditions at 25°C, *Pdf* mutants show increased sleep during the day, as well as during the subjective day under

constant conditions (*66*). However, the effect of *Pdf* loss on sleep appears to be dependent on temperature: These flies show increased sleep at 25°C and decreased sleep at 18°C (Fig. 5L). We analyzed the sleep profiles of flies expressing *hid* in the SLP316 cells under an LD cycle at 25°C and observed a significant increase in daytime sleep (Fig. 6, A and B). [These results were obtained using the standard quantification based on periods of 5 min of inactivity (*68*, *69*)]. A similar phenotype was observed in *SLP316 > TNT* flies (Fig. 6, E and F). Experimental females showed similar sleep phenotypes (fig. S4, F to K). These findings allow us to conclude that the effects on sleep are not unique to low-temperature cycles but, in contrast to PDF's temperature-dependent roles, reflect a feature of the SLP316 neurons at both low and high temperatures.

To determine the underlying cause for this increase in sleep, we analyzed *P*(doze) and *P*(wake), the probabilities that an inactive fly will start moving or an active fly will stop moving, respectively, between 1-min activity bins. *P*(doze) corresponds to sleep pressure, and *P*(wake) corresponds to sleep depth; thus, these conditional probabilities can offer insights into the biological processes driving changes in sleep (*70*). We found that *P*(doze) was higher throughout most of the day and night for both *SLP316 > hid* and *SLP316 > TNT* animals, especially during the evening (ZT6 to ZT12) and morning (ZT18 to ZT3), when flies are most active (Fig. 6, C, D, G, and H). The average *P*(wake) was not significantly affected in either manipulation, although *SLP316 > hid* flies showed a minor reduction in *P*(wake) when compared to that at ZT9 to ZT12 (fig. S8, A to D). This increase in *P*(doze) suggests that the increased sleep observed when the SLP316s are silenced was due to increased sleep pressure, especially at times when flies would be most active. Sleep in *Drosophila* is typically defined as 5 min of inactivity, though recent studies suggest that longer bouts may more accurately reflect sleep states (*71*–*73*). Analysis of longer sleep bouts (60 min) revealed an increase in daytime sleep in *SLP316 > TNT*, but not *SLP316 > hid*, flies (fig. S8, E and F). Expression of *NaChBac* in SLP316 neurons did not change daytime or nighttime sleep (fig. S8, G to I). *P*(doze) values were not significantly different from those of controls at any specific time points but were higher when total values across the entire recording period were compared; *P*(wake) values were not affected (fig. S8, J to M). We conclude that silencing SLP316 neurons caused an increase in daytime sleep under both 25°C and low-temperature conditions and that this phenotype is not dependent on PDF because manipulations of *Pdf* led to opposite phenotypes.

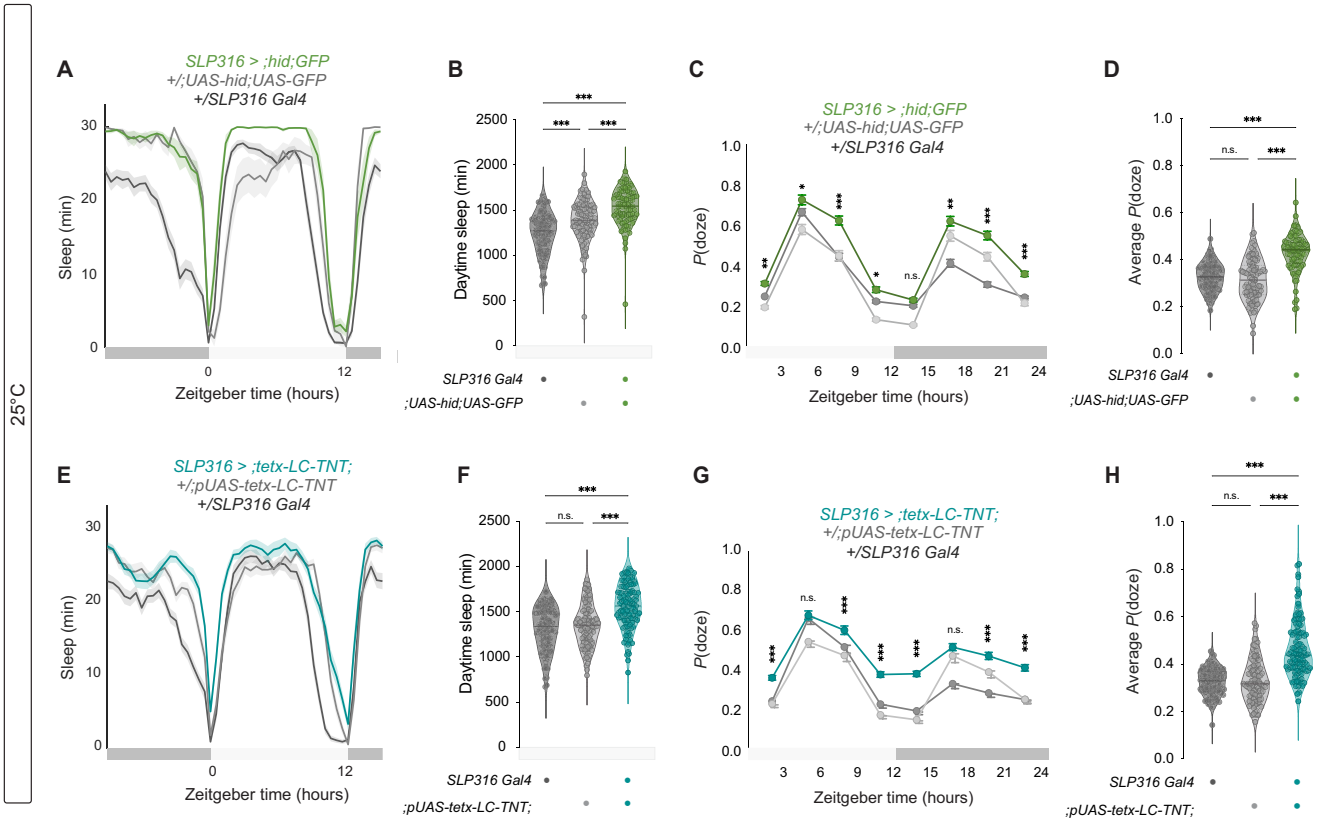

Fig. 6. Silencing or eliminating SLP316 neurons increased the amount of daytime sleep. (**A**) Representative sleep plot averaged from 3 days of 12-hour:12-hour LD cycle at 25°C for control (*SLP316 split-GAL4* and *;UAS-hid;UAS-GFP*) and experimental (*SLP316 > ;hid;GFP*) flies. (**B**) Total daytime sleep over 3 days for each genotype. (**C**) Representative sleep plot and (**D**) total daytime sleep for control (*SLP316-Gal4* and *;pUAS-tetx-LC-TNT;*) and experimental (*SLP316 > tetx-LC-TNT*) flies. (**E**) *P*(doze) from the same 3 days of LD, plotted in 3-hour bins for controls (*SLP316 split-GAL4* and *;UAS-hid;UAS-GFP*) and experimental (*SLP316 > ;hid;GFP*) flies. (**F**) Average *P*(doze) throughout the entire 3-day period. (**G**) *P*(doze) plot and (**H**) average *P*(doze) for control (*SLP316-Gal4* and *;pUAS-tetx-LC-TNT;*) and experimental (*SLP316 > tetx-LC-TNT*) flies under the same conditions. Sleep was quantified using PHASE based on periods of inactivity of 5 min or more and plotted in (A) and (C) as minutes of sleep per 30-min bin. *P*(doze) was quantified in R using routines from the Griffith Laboratory (*70*). Statistical comparisons were conducted using the Kruskal-Wallis test, followed by Dunn's multiple comparisons test. Data are plotted from four replicate experiments. **P* < 0.05, ***P* < 0.01, ****P* < 0.001.

DISCUSSION

The recent availability of connectomic data allows the identification of neuronal connections that have not been described using other approaches. We used openly available *Drosophila* connectomes to identify the SLP316 neurons, which are the main postsynaptic partners of the sLN_vs, the key pacemaker neurons in the *Drosophila* clock network. We found that genetic manipulations of the SLP316 neurons led to small but robust changes in free-running rhythms: Silencing their activity via TNT or eliminating them via *hid* led to a period shortening, whereas hyperexciting them via *NaChBac* led to a period lengthening. Another important behavioral output of the sLN_vs, eclosion rhythm, was not affected by the elimination of SLP316 neurons. Under LD cycles, silencing SLP316s resulted in a reduction in daytime activity and an increase in sleep, under both 25°C and low-temperature conditions. Neither the free-running nor the LD phenotypes observed following SLP316 manipulations resembled those caused by the loss of PDF, a well-known output of the sLN_vs, which facilitates communication with the rest of the circadian clock network.

Our study identified a nonclock group of neurons that affects circadian rhythms and contributes to our understanding of neuronal connectivity within the clock network. To date, the best characterized output of the sLN_vs is PDF (*18*, *74*), a neuropeptide that accumulates—and is also released (*34*)—rhythmically from their dorsal termini and soma, likely independently of classical transmitter release from these cells (*33*). The sLN_vs also express sNPF (*28*), and there is evidence that they also use glycine to communicate with postsynaptic targets (*32*). On the basis of the availability of neurotransmitter use information, the flywire electron microscopy (EM) prediction for the sLN_vs is acetylcholine (*51*), but the likelihood is relatively low.

The sLN_vs and two other groups of clock neurons (DN2 and DN1a) are born early in development, during the early larval stage (*75*–*78*). Their cell number remains stable throughout adulthood, with projections innervating the dorsal posterior brain (*64*). Our results show that the number of SLP316 cells is higher immediately after eclosion (~3.8) compared to 1-week-old flies (~2.9), and it is possible that the strength of the connections between the sLN_vs cells and the SLP316s changes over time. Another group of PDF^+ neurons, which are located in the anterior protocerebrum and are called PDF-tri, also extends their projections toward the area where the sLN_v dorsal termini and the SLP316 reside (*64*). These neurons extend their projections along the midline and innervate the pars intercerebralis and lateralis, with some neurites contacting the dorsal termini of the sLN_vs (*64*). This is a developmentally transient population that undergoes programmed cell death ~4 days after eclosion (*64*, *79*). Similar to small LN_vs, PDF-tri neurons have PDF-positive dense-core vesicles along with PDF-negative small clear vesicles (*80*) and have been proposed to be neuromodulatory (*79*). It is possible that during metamorphosis, or shortly after eclosion, these cells also form transient synapses onto the SLP316 cells. We did not observe any eclosion rhythm phenotypes following manipulation of SLP316 neurons; however, they may play roles in other developmental processes. Functional connectivity experiments targeting the sLN_vs and SLP316 neurons at different developmental stages may help elucidate the dynamics and functional relevance of their interaction.

Given their prominent role in the clock network, several studies have examined neuronal targets of the sLN_vs that could contribute to the propagation of rhythmic signals throughout the brain. PDFRs (*PdfR*) are expressed by a wide range of neurons distributed throughout the brain, including much of the clock network (*6*), and PDFR-expressing cells respond to sLN_v stimulation (*81*). sLN_vs also express sNPF, and PTTH neurons, which are downstream of sLN_vs, express sNPF receptors and are inhibited by the sLN_vs via sNPF to regulate eclosion rhythms (*31*). Connections between Pdf^+ cells and nonclock cells that regulate rhythm amplitude were detected via GFP Reconstitution Across Synaptic Partners (GRASP) (*82*). More recently, the Blau laboratory used the transsynaptic tracer trans-Tango to identify neuronal populations downstream of the sLN_vs and reported that they form connections with a subset of DN1p clock neurons that express the neuropeptide CNMa and with mushroom body Kenyon cells (*83*). Strong monosynaptic connections between the sLN_vs and the DN1ps cannot be detected in the connectomes (*16*, *50*), but it is possible that those synapses were missed because the sLN_vs show daily structural plasticity rhythms (*84*), as do the vasoactive intestinal peptide–expressing neurons in the SCN (*85*). Truncation of the dorsal termini of the sLN_vs, which are the sites of synaptic output and undergo clock-controlled plasticity, does not affect free-running rhythms (*39*, *86*), suggesting that PDF release is independent of the arborization rhythms. In addition, silencing synaptic transmission in Pdf^+ neurons via TNT does not lead to the loss of behavioral rhythms (*36*) or the down-regulation of *brp* or other active zone proteins (*33*). Together, these results suggest that, unlike PDF release, the synaptic connections that the sLN_vs form with downstream neurons are not required for maintaining activity-rest rhythms under free-running conditions. However, those connections play a role in regulating the free-running period of those rhythms.

The sLN_vs appear to contact the DN1p clock neurons both via PDF release (*60*) and synaptically through the SLP316s (Fig. 1). A functional clock in CRYPTOCHROME (CRY)-positive DN1ps, along with the presence of PDF, is sufficient for morning anticipation (*45*, *46*, *87*). Neither inhibition of synaptic transmission from sLN_v nor manipulation of the SLP316 cells appeared to affect morning anticipation, suggesting that this feature depends only on PDF signaling from the sLN_vs. Rescuing the molecular clock in a glutamatergic subset of DN1ps can promote an evening peak of activity when PDF is reduced or absent (*45*, *65*). The pronounced and very early peak of activity we observed in Pdf^{01} flies under cold temperatures may at least, in part, be due to increased prominence of the activity of evening DN1ps in the absence of PDF (*88*). Another clock subset, DN1a, which is inhibited by cold temperature, is reciprocally connected to the sLN_vs through the neuropeptides CCHamide1 and PDF (*89*, *90*). Thus, a cold temperature–induced change in sLN_v activity could alter evening DN1p activity via the SLP316s, while simultaneous loss of PDF eliminates suppression of the DN1p-induced effects. These glutamatergic DN1ps are also sleep promoting; activating them increases daytime sleep and the arousal threshold between ZT6 and ZT10, whereas inhibiting them decreases both daytime and nighttime sleep (*91*). If the SLP316 neurons are glutamatergic as predicted in Flywire (*50*) and inhibitory, then silencing them would be expected to increase the neuronal activity of the DN1ps and thus daytime sleep levels, in agreement with our results.

Studying how neurons use different signals to communicate with downstream targets is essential for understanding how networks of neurons produce behavior. The *Drosophila* sLN_vs are an excellent model for studying the neuronal basis of behavior, given their well-characterized role as key circadian pacemakers. This role relies on their release of the neuropeptide PDF as a critical output signal for synchrony within the network. Our study is the first to examine the role in rhythmic behavior of direct synaptic targets of the sLN_vs

based on connectomic data, a connection that is likely independent of PDF. Our results reveal that manipulations of the SLP316 cells, the primary postsynaptic partners of the sLN_vs in the connectome, can affect the free-running period, which is a core circadian parameter. This finding indicates that a nonclock neuronal cell type can modulate circadian timekeeping. In addition, we show that manipulations of the SLP316 cells and the loss of PDF lead to different behavioral phenotypes, both under free-running conditions and standard and low-temperature LD cycles. These two output pathways of the clock neuron may add plasticity to the system and allow the circadian network to adjust to changing environmental conditions.

MATERIALS AND METHODS

Fly lines and husbandry

Flies were reared on cornmeal-sucrose-yeast medium under a 12-hour: 12-hour LD cycle at 25°C. The fly lines used in this study were *SLP316 split-GAL4* (SS76489: w; 38E08-p65ADZp in attP40; 36B07-ZpGdbd in attP2), *w; Pdf-Red, Pdf-Gal4; w;;UAS-NaChBac, w;UAS-hid/cyo;UAS-mCD8-GFP, w;UAS-TeTxLC;, w^{1118}, w;;Pdf^{01}*, and *w;* LexAop2-Syb.GFPN146I.TEVT173V LexAop2-QF2.V5.hSNAP25.HIVNES.Syx1A/CyO,20XUAS-B3R.PEST-UAS(B3RT.B2)BoNTA QUAS-mtdTomato-3xHA/TM6B, Tb1 (see the "Fly Lines and reagents" table for details).

We identified the SLP316 *split-GAL4* line (SS76489) by screening candidate hemidriver combinations selected by comparing GAL4 driver expression patterns and the hemibrain reconstructions of SLP316. This work was done in collaboration with the Janelia FlyLight Project Team using established methods, and the driver line is included in a recently published *split-GAL4* collection (*92*).

Immunohistochemistry

Flies were entrained to 12-hour:12-hour LD cycles at 25°C and dissected at the specified times in cold Schneider's *Drosophila* Medium. For all experiments, dissections were completed within 30 min. For anti-PER staining (Fig. 2D), brains were dissected at ZT23 on the fifth day under LD. Brains were fixed in 2% paraformaldehyde prepared in Schneider's *Drosophila* Medium for 30 min at room temperature. Blocking was performed using 5% normal goat serum in phosphate-buffered saline (PBS) containing 0.3% Triton X-100 (PBS-TX) for 1 hour at room temperature. Samples were incubated with primary antibodies for 24 to 48 hours at 4°C, followed by several washes with PBS-TX under agitation. Secondary antibody cocktails were applied for 24 to 48 hours at 4°C, after which samples were washed again with PBS-TX. Antibodies (see Table 2) were diluted in PBS-TX supplemented with 5% normal goat serum. Brains were mounted between coverslips and imaged at the Advanced Science Research Center using an Olympus Fluoview 3000 laser-scanning confocal microscope (Olympus, Center Valley, PA). SLP316 cell bodies were quantified from all intact hemispheres of 1- and 7-day-old males and females using a 40× objective. Brains for the BAcTrace experiments were imaged using an Olympus/Evident Fluoview 4000 laser-scanning confocal microscope (Fernández Lab, Indiana University Bloomington).

Image analysis

Hr38-Tomato intensity was calculated using the Fiji platform in ImageJ. sLN_v or SLP316 cell bodies were identified from the PDF or GFP signal, respectively, using the "Thermal" lookup table. The highest local RFP intensity in the Z-series was recorded from a 4.5-μm region of interest encompassing each sLN_v or SLP316 cell body (see fig. S2), and intensities were averaged across the hemisphere with background correction. Corrected intensities between hemispheres in a brain were averaged when applicable. Cosinor analysis was implemented using the CRAN Cosinor package in R.

The light microscopy (LM) images in fig. S2 are based on confocal stacks previously reported (*92*), and the original images are available online (https://splitgal4.janelia.org/cgi-bin/view_splitgal4_imagery.cgi?line=SS76489). The EM-LM overlay was generated using VVD-Viewer (https://zenodo.org/records/14468001). The other images show maximum intensity projections produced using Fiji (https://imagej.net/software/fiji/).

Connectome analysis

The *Drosophila* Hemibrain (release v2.1) was accessed via Neuprint (https://neuprint.janelia.org/). FlyWire data are based on FAFB version 783 (https://flywire.ai/) (*50*, *93*). Hemibrain reconstructions are identified by their instance names in Neuprint (e.g., "SLP316_R") with individual cells distinguished here by an additional number ("SLP316_R_1").

Behavior recording and analysis

Locomotor activity rhythms of adult male and virgin female flies were recorded using DAM2 *Drosophila* Activity Monitors. Three- to six-day-old flies were placed individually in TriKinetics capillary tubes containing 2% agar–4% sucrose food at one end sealed with a cap, plugged with a small length of yarn, and loaded into the DAM2 monitors for locomotor activity recording. Flies were entrained to 12-hour:12-hour LD cycles for at least 5 days and then released into DD for at least 9 days at a constant temperature of 18° or 25°C (as indicated in the figure legend for each experiment). For *shibire*^{ts} experiments, flies were raised at 19°C and either kept at that temperature or transferred to 29°C immediately upon eclosion. Behavior experiments were conducted at 19° or 29°C, respectively.

Free-running activity rhythms were analyzed with ClockLab software. ClockLab's chi-square periodogram function was used to analyze rhythmicity and rhythmic power in individual flies using 30-min bins for activity and a confidence level of 0.01. The "rhythmic power" for each designated rhythmic fly was determined by subtracting the "significance" value from the "power" value associated with the predominant peak. Flies that did not exhibit a rhythmic power of 10 were categorized as "arrhythmic," and their period and rhythmic power were not included in the analysis (*94*). ClockLab periodogram analysis was repeated for rhythmic flies using 1-min bins to quantify free-running period. For each of the genotypes tested, only periodicities falling within the 14- to 34-hour range were considered. Phases on the eighth day of free running were calculated using 1-min bins and applying a least-squares sine-wave fit in the ClockLab activity profile, excluding any phases with $P > 0.05$. All relevant information about statistical analyses is included in table S1.

Activity counts were collected in 1-min bins and averaged across the population; profiles of specific genotypes under LD were generated using PHASE (*95*). To do so, the activity levels of each fly were first normalized by establishing the average activity across all 30-min bins over days 2 to 4 under LD. Population averages of this normalized activity were computed for each 30-min bin and averaged into a single representative 24-hour day. Total daytime (ZT0 to ZT12) and nighttime (ZT12 to ZT24) activity counts from days 2 to 4 of LD were recorded. Representative sleep plots and amounts were similarly generated for LD

days 2 to 4 by classifying 5-min periods of inactivity as sleep, unless otherwise specified. Total daytime and nighttime sleep over the 3-day period were also recorded. Morning and evening phases were quantified in PHASE using a filter frame length of 481 min and filter order of 2. *P*(wake) and *P*(doze) values (*70*) were averaged for the entire duration of LD days 2 to 4 or in 3-hour windows and across the same days.

Adult emergence monitoring

Flies were raised at 25°C for 5 days, then transferred to 20°C, and entrained under a 12-hour:12-hour LD cycle. Resulting pupae were collected and fixed on eclosion plates with Elmer's glue and mounted on TriKinetics eclosion monitors (TriKinetics, MA, USA). Emergence was then monitored for 7 days at 20°C under DD conditions and analyzed as previously described (*96*). Rhythmicity of eclosion profiles was analyzed using MATLAB (MathWorks Inc., Natick) and the appropriate MATLAB toolbox (*97*). Using autocorrelation analyses, records were considered rhythmic if the rhythmicity index (RI) was 0.3, weakly rhythmic if RI < 0.3, and arrhythmic if RI < 0.1 (*20*).

Statistical analysis

Statistical tests were performed on GraphPad Prism (v.10.4.0), with the specific tests used detailed in the figure legends. A P value of < 0.05 was considered statistically significant. Details of statistical analyses for all reported experiments are provided in table S1.

Fly lines and reagents

See Table 2.

Table 2. Fly lines and reagents.

Reagent or resource	Source	Identifier
Experimental models: Organisms/strains		
SLP316 split-GAL4 (w; 38E08-p65ADZp in attP40; 36B07-ZpGdbd in attP2)	G. Rubin and A.N., HHMI, Janelia Research Campus	SS76489
w;Pdf-Red,Pdf-Gal4/Cyo;	Justin Blau, New York University	(*98*)
w;;UAS-NaChBac	Bloomington Drosophila Stock Center	RRID: BDSC_9468
yw;UAS-hid/CyO;	Bloomington Drosophila Stock Center	RRID: BDSC_1557
w; UAS-TeTxLC;	C. O'Kane, University of Cambridge	RRID: BDSC_28838
w;UAS-rpr;	Bloomington Drosophila Stock Center	RRID: BDSC_5824
w^{1118};+;+	Bloomington Drosophila Stock Center	RRID: BDSC_3605
w;;Pdf^{01}	P. Taghert, Washington Univ. Med. School	(*18*)
w;;UAS-shibire^{ts}	Bloomington Drosophila Stock Center	RRID: BDSC_44222
LexAop2-Syb.GFPN146I.TEVT173V LexAop2QF2.V5.hSNAP25.HIVNES.Syx1A/CyO, 20XUAS-B3R.PEST UAS(B3RT.B2)BoNTA QUAS-mtdTomato-3xHA/TM6B, Tb1	Bloomington Drosophila Stock Center	RRID: BDSC 90825
Antibodies		
Mouse anti-PDF (1:3,000 or 1:2,000)	Developmental Studies Hybridoma Bank	
Rabbit anti-GFP (1:2,000)	Thermo Fisher Scientific	A-11122
Rat anti-PER (1:500)	O. Shafer, Indiana University Bloomington	
Rabbit anti-RFP (1:2,000)	Rockland	#600-401-379-RTU
Chicken anti-GFP (1:2,000)	Rockland	#600-901-215
Anti-mouse Alexa Fluor 488 (1:3,000)	Thermo Fisher Scientific	A11029
Anti-rabbit Alexa Fluor 488 (1:3,000)	Thermo Fisher Scientific	A48282
Anti-rat Alexa Fluor 568 (1:3,000)	Thermo Fisher Scientific	A78946
Anti-rabbit Alexa Fluor 568 (1:3,000)	Thermo Fisher Scientific	A11036
Anti-chicken Alexa Fluor 488 (1:3,000)	Thermo Fisher Scientific	A11039
Software		
Fiji	http://fiji.sc	RRID: SCR_002285
PHASE	Open-source software: https://github.com/ajlopatkin/PHASE	(*95*)
MATLAB R2022b	MathWorks, Natick	RRID: SCR_001622
GraphPad Prism 9.0	GraphPad Software	RRID: SCR_002798
DAM FileScan	TriKinetics	
ClockLab	Actimetrics	RRID: SCR_014309
Chemicals		
VECTASHIELD Mounting Medium	Vector Laboratories	#H-1000-10

Supplementary Materials

The PDF file includes:
Figs. S1 to S8
Legends for tables S1 and S2

Other Supplementary Material for this manuscript includes the following:
Tables S1 and S2

REFERENCES AND NOTES

1. E. D. Herzog, Neurons and networks in daily rhythms. *Nat. Rev. Neurosci.* **8**, 790–802 (2007).
2. D. K. Welsh, J. S. Takahashi, S. A. Kay, Suprachiasmatic nucleus: Cell autonomy and network properties. *Annu. Rev. Physiol.* **72**, 551–577 (2010).
3. M. H. Hastings, M. Brancaccio, E. S. Maywood, Circadian pacemaking in cells and circuits of the suprachiasmatic nucleus. *J. Neuroendocrinol.* **26**, 2–10 (2014).
4. E. S. Maywood, J. E. Chesham, J. A. O'Brien, M. H. Hastings, A diversity of paracrine signals sustains molecular circadian cycling in suprachiasmatic nucleus circuits. *Proc. Natl. Acad. Sci. U.S.A.* **108**, 14306–14311 (2011).
5. B. Ananthasubramaniam, E. D. Herzog, H. Herzel, Timing of neuropeptide coupling determines synchrony and entrainment in the mammalian circadian clock. *PLOS Comput. Biol.* **10**, e1003565 (2014).
6. P. H. Taghert, M. N. Nitabach, Peptide neuromodulation in invertebrate model systems. *Neuron* **76**, 82–97 (2012).
7. D. R. Nässel, M. Zandawala, Recent advances in neuropeptide signaling in *Drosophila*, from genes to physiology and behavior. *Prog. Neurobiol.* **179**, 101607 (2019).
8. N. Reinhard, A. Fukuda, G. Manoli, E. Derksen, A. Saito, G. Möller, M. Sekiguchi, D. Rieger, C. Helfrich-Förster, T. Yoshii, M. Zandawala, Synaptic connectome of the *Drosophila* circadian clock. *Nat. Commun.* **15**, 10392 (2024).
9. C. Helfrich-Förster, N. Reinhard, Mutual coupling of neurons in the circadian master clock: What we can learn from fruit flies. *Neurobiol. Sleep Circadian Rhythms* **18**, 100112 (2025).
10. C. Helfrich-Forster, The neuroarchitecture of the circadian clock in the brain of *Drosophila melanogaster*. *Microsc. Res. Tech.* **62**, 94–102 (2003).
11. F. K. Schubert, N. Hagedorn, T. Yoshii, C. Helfrich-Forster, D. Rieger, Neuroanatomical details of the lateral neurons of *Drosophila melanogaster* support their functional role in the circadian system. *J. Comp. Neurol.* **526**, 1209–1231 (2018).
12. C. Dubowy, A. Sehgal, Circadian rhythms and sleep in *Drosophila melanogaster*. *Genetics* **205**, 1373–1397 (2017).
13. C. Helfrich-Forster, Organization of endogenous clocks in insects. *Biochem. Soc. Trans.* **33**, 957–961 (2005).
14. D. Ma, D. Przybylski, K. C. Abruzzi, M. Schlichting, Q. Li, X. Long, M. Rosbash, A transcriptomic taxonomy of *Drosophila* circadian neurons around the clock. *eLife* **10**, e63056 (2021).
15. O. T. Shafer, C. Helfrich-Forster, S. C. Renn, P. H. Taghert, Reevaluation of *Drosophila melanogaster*'s neuronal circadian pacemakers reveals new neuronal classes. *J. Comp. Neurol.* **498**, 180–193 (2006).
16. O. T. Shafer, G. J. Gutierrez, K. Li, A. Mildenhall, D. Spira, J. Marty, A. A. Lazar, M. P. Fernandez, Connectomic analysis of the *Drosophila* lateral neuron clock cells reveals the synaptic basis of functional pacemaker classes. *eLife* **11**, e79139 (2022).
17. X. Liang, T. E. Holy, P. H. Taghert, Synchronous *Drosophila* circadian pacemakers display nonsynchronous Ca^{2+} rhythms in vivo. *Science* **351**, 976–981 (2016).
18. S. C. Renn, J. H. Park, M. Rosbash, J. C. Hall, P. H. Taghert, A *pdf* neuropeptide gene mutation and ablation of PDF neurons each cause severe abnormalities of behavioral circadian rhythms in *Drosophila*. *Cell* **99**, 791–802 (1999).
19. J. H. Park, C. Helfrich-Forster, G. Lee, L. Liu, M. Rosbash, J. C. Hall, Differential regulation of circadian pacemaker output by separate clock genes in *Drosophila*. *Proc. Natl. Acad. Sci. U.S.A.* **97**, 3608–3613 (2000).
20. B. Grima, E. Chelot, R. Xia, F. Rouyer, Morning and evening peaks of activity rely on different clock neurons of the *Drosophila* brain. *Nature* **431**, 869–873 (2004).
21. D. Stoleru, Y. Peng, J. Agosto, M. Rosbash, Coupled oscillators control morning and evening locomotor behaviour of *Drosophila*. *Nature* **431**, 862–868 (2004).
22. T. Yoshii, C. Wulbeck, H. Sehadova, S. Veleri, D. Bichler, R. Stanewsky, C. Helfrich-Forster, The neuropeptide pigment-dispersing factor adjusts period and phase of *Drosophila's* clock. *J. Neurosci.* **29**, 2597–2610 (2009).
23. Y. Peng, D. Stoleru, J. D. Levine, J. C. Hall, M. Rosbash, *Drosophila* free-running rhythms require intercellular communication. *PLOS Biol.* **1**, E13 (2003).
24. X. Liang, T. E. Holy, P. H. Taghert, A series of suppressive signals within the *Drosophila* circadian neural circuit generates sequential daily outputs. *Neuron* **94**, 1173–1189.e4 (2017).
25. I. Mertens, A. Vandingenen, E. C. Johnson, O. T. Shafer, W. Li, J. S. Trigg, A. De Loof, L. Schoofs, P. H. Taghert, PDF receptor signaling in *Drosophila* contributes to both circadian and geotactic behaviors. *Neuron* **48**, 213–219 (2005).
26. S. Hyun, Y. Lee, S. T. Hong, S. Bang, D. Paik, J. Kang, J. Shin, J. Lee, K. Jeon, S. Hwang, E. Bae, J. Kim, *Drosophila* GPCR Han is a receptor for the circadian clock neuropeptide PDF. *Neuron* **48**, 267–278 (2005).
27. B. C. Lear, C. E. Merrill, J. M. Lin, A. Schroeder, L. Zhang, R. Allada, A G protein-coupled receptor, groom-of-PDF, is required for PDF neuron action in circadian behavior. *Neuron* **48**, 221–227 (2005).
28. H. A. D. Johard, T. Yoishii, H. Dircksen, P. Cusumano, F. Rouyer, C. Helfrich-Förster, D. R. Nässel, Peptidergic clock neurons in *Drosophila*: Ion transport peptide and short neuropeptide F in subsets of dorsal and ventral lateral neurons. *J. Comp. Neurol.* **516**, 59–73 (2009).
29. C. G. Vecsey, N. Pirez, L. C. Griffith, The *Drosophila* neuropeptides PDF and sNPF have opposing electrophysiological and molecular effects on central neurons. *J. Neurophysiol.* **111**, 1033–1045 (2014).
30. Y. Shang, N. C. Donelson, C. G. Vecsey, F. Guo, M. Rosbash, L. C. Griffith, Short neuropeptide F is a sleep-promoting inhibitory modulator. *Neuron* **80**, 171–183 (2013).
31. M. Selcho, C. Millán, A. Palacios-Muñoz, F. Ruf, L. Ubillo, J. Chen, G. Bergmann, C. Ito, V. Silva, C. Wegener, J. Ewer, Central and peripheral clocks are coupled by a neuropeptide pathway in *Drosophila*. *Nat. Commun.* **8**, 15563 (2017).
32. L. Frenkel, N. I. Muraro, A. N. Beltran Gonzalez, M. S. Marcora, G. Bernabo, C. Hermann-Luibl, J. I. Romero, C. Helfrich-Forster, E. M. Castano, C. Marino-Busjle, D. J. Calvo, M. F. Ceriani, Organization of circadian behavior relies on glycinergic transmission. *Cell Rep.* **19**, 72–85 (2017).
33. B. Hofbauer, M. Zandawala, N. Reinhard, D. Rieger, C. Werner, J. F. Evers, C. Wegener, The neuropeptide pigment-dispersing factor signals independently of Bruchpilot-labelled active zones in daily remodelled terminals of *Drosophila* clock neurons. *Eur. J. Neurosci.* **59**, 2665–2685 (2024).
34. M. K. Klose, M. P. Bruchez, D. L. Deitcher, E. S. Levitan, Temporally and spatially partitioned neuropeptide release from individual clock neurons. *Proc. Natl. Acad. Sci. U.S.A.* **118**, e2101818118 (2021).
35. S. T. Sweeney, K. Broadie, J. Keane, H. Niemann, C. J. O'Kane, Targeted expression of tetanus toxin light chain in *Drosophila* specifically eliminates synaptic transmission and causes behavioral defects. *Neuron* **14**, 341–351 (1995).
36. M. Kaneko, J. H. Park, Y. Cheng, P. E. Hardin, J. C. Hall, Disruption of synaptic transmission or clock-gene-product oscillations in circadian pacemaker cells of *Drosophila* cause abnormal behavioral rhythms. *J. Neurobiol.* **43**, 207–233 (2000).
37. A. R. Iyer, E. Scholz-Carlson, E. Bell, G. Biondi, S. Richhariya, M. P. Fernandez, Circadian rhythms are more resilient to pacemaker neuron disruption in female *Drosophila*. *PLOS Biol.* **23**, e3003146 (2025).
38. M. P. Brown, S. Verma, I. Palmer, A. G. Zuniga, C. Rosensweig, M. F. Keles, M. N. Wu, A subclass of evening cells promotes the switch from arousal to sleep at dusk. bioRxiv 555147 [Preprint] (2023). https://doi.org/10.1101/2023.08.28.555147.
39. M. P. Fernandez, H. L. Pettibone, J. T. Bogart, C. J. Roell, C. E. Davey, A. Pranevicius, K. V. Huynh, S. M. Lennox, B. S. Kostadinov, O. T. Shafer, Sites of circadian clock neuron plasticity mediate sensory integration and entrainment. *Curr. Biol.* **30**, 2225–2237.e5 (2020).
40. F. Guo, X. Chen, M. Rosbash, Temporal calcium profiling of specific circadian neurons in freely moving flies. *Proc. Natl. Acad. Sci. U.S.A.* **114**, E8780–E8787 (2017).
41. A. Lamaze, R. Stanewsky, DN1p or the "Fluffy" cerberus of clock outputs. *Front. Physiol.* **10**, 1540 (2019).
42. B. Collins, E. A. Kane, D. C. Reeves, M. H. Akabas, J. Blau, Balance of activity between LN_vs and glutamatergic dorsal clock neurons promotes robust circadian rhythms in *Drosophila*. *Neuron* **74**, 706–718 (2012).
43. J. Majercak, D. Sidote, P. E. Hardin, I. Edery, How a circadian clock adapts to seasonal decreases in temperature and day length. *Neuron* **24**, 219–230 (1999).
44. P. Lamba, L. E. Foley, P. Emery, Neural network interactions modulate CRY-dependent photoresponses in *Drosophila*. *J. Neurosci.* **38**, 6161–6171 (2018).
45. A. Chatterjee, A. Lamaze, J. De, W. Mena, E. Chelot, B. Martin, P. Hardin, S. Kadener, P. Emery, F. Rouyer, Reconfiguration of a multi-oscillator network by light in the *Drosophila* circadian clock. *Curr. Biol.* **28**, 2007–2017.e4 (2018).
46. Y. Zhang, Y. Liu, D. Bilodeau-Wentworth, P. E. Hardin, P. Emery, Light and temperature control the contribution of specific DN1 neurons to *Drosophila* circadian behavior. *Curr. Biol.* **20**, 600–605 (2010).
47. K. M. Parisky, J. L. Agosto Rivera, N. C. Donelson, S. Kotecha, L. C. Griffith, Reorganization of sleep by temperature in *Drosophila* requires light, the homeostat, and the circadian clock. *Curr. Biol.* **26**, 882–892 (2016).
48. C. Kistenpfennig, R. Grebler, M. Ogueta, C. Hermann-Luibl, M. Schlichting, R. Stanewsky, P. R. Senthilan, C. Helfrich-Forster, A new rhodopsin influences light-dependent daily activity patterns of fruit flies. *J. Biol. Rhythms* **32**, 406–422 (2017).
49. L. K. Scheffer, C. S. Xu, M. Januszewski, Z. Lu, S. Y. Takemura, K. J. Hayworth, G. B. Huang, K. Shinomiya, J. Maitlin-Shepard, S. Berg, J. Clements, P. M. Hubbard, W. T. Katz, L. Umayam, T. Zhao, D. Ackerman, T. Blakely, J. Bogovic, T. Dolafi, D. Kainmueller, T. Kawase, K. A. Khairy, L. Leavitt, P. H. Li, L. Lindsey, N. Neubarth, D. J. Olbris, H. Otsuna,

E. T. Trautman, M. Ito, A. S. Bates, J. Goldammer, T. Wolff, R. Svirskas, P. Schlegel, E. Neace, C. J. Knecht, C. X. Alvarado, D. A. Bailey, S. Ballinger, J. A. Borycz, B. S. Canino, N. Cheatham, M. Cook, M. Dreher, O. Duclos, B. Eubanks, K. Fairbanks, S. Finley, N. Forknall, A. Francis, G. P. Hopkins, E. M. Joyce, S. Kim, N. A. Kirk, J. Kovalyak, S. A. Lauchie, A. Lohff, C. Maldonado, E. A. Manley, S. McLin, C. Mooney, M. Ndama, O. Ogundeyi, N. Okeoma, C. Ordish, N. Padilla, C. M. Patrick, T. Paterson, E. E. Phillips, E. M. Phillips, N. Rampally, C. Ribeiro, M. K. Robertson, J. T. Rymer, S. M. Ryan, M. Sammons, A. K. Scott, A. L. Scott, A. Shinomiya, C. Smith, K. Smith, N. L. Smith, M. A. Sobeski, A. Suleiman, J. Swift, S. Takemura, I. Talebi, D. Tarnogorska, E. Tenshaw, T. Tokhi, J. J. Walsh, T. Yang, J. A. Horne, F. Li, R. Parekh, P. K. Rivlin, V. Jayaraman, M. Costa, G. S. Jefferis, K. Ito, S. Saalfeld, R. George, I. A. Meinertzhagen, G. M. Rubin, H. F. Hess, V. Jain, S. M. Plaza, A connectome and analysis of the adult *Drosophila* central brain. *eLife* **9**, e57443 (2020).

50. S. Dorkenwald, A. Matsliah, A. R. Sterling, P. Schlegel, S.-c. Yu, C. E. McKellar, A. Lin, M. Costa, K. Eichler, Y. Yin, W. Silversmith, C. Schneider-Mizell, C. S. Jordan, D. Brittain, A. Halageri, K. Kuehner, O. Ogedengbe, R. Morey, J. Gager, K. Kruk, E. Perlman, R. Yang, D. Deutsch, D. Bland, M. Sorek, R. Lu, T. Macrina, K. Lee, J. A. Bae, S. Mu, B. Nehoran, E. Mitchell, S. Popovych, J. Wu, Z. Jia, M. A. Castro, N. Kemnitz, D. Ih, A. S. Bates, N. Eckstein, J. Funke, F. Collman, D. D. Bock, G. S. X. E. Jefferis, H. S. Seung, M. Murthy, Z. Lenizo, A. T. Burke, K. P. Willie, N. Serafetinidis, N. Hadjerol, R. Willie, B. Silverman, J. A. Ocho, J. Bañez, R. A. Candilada, A. Kristiansen, N. Panes, A. Yadav, R. Tancontian, S. Serona, J. I. Dolorosa, K. J. Vinson, D. Garner, R. Salem, A. Dagohoy, J. Skelton, M. Lopez, L. S. Capdevila, G. Badalamente, T. Stocks, A. Pandey, D. J. Akiatan, J. Hebditch, C. David, D. Sapkal, S. M. Monungolh, V. Sane, M. L. Pielago, M. Albero, J. Laude, M. dos Santos, Z. Vohra, K. Wang, A. M. Gogo, E. Kind, A. J. Mandahay, C. Martinez, J. D. Asis, C. Nair, D. Patel, M. Manaytay, I. F. M. Tamimi, C. A. Lim, P. L. Ampo, M. D. Pantujan, A. Javier, D. Bautista, R. Rana, J. Seguido, B. Parmar, J. C. Saguimpa, M. Moore, M. W. Pleijzier, M. Larson, J. Hsu, I. Joshi, D. Kakadiya, A. Braun, C. Pilapil, M. Gkantia, K. Parmar, Q. Vanderbeck, I. Salgarella, C. Dunne, E. Munnelly, C. H. Kang, L. Lörsch, J. Lee, L. Kmecova, G. Sancer, C. Baker, J. Joroff, S. Calle, Y. Patel, O. Sato, S. Fang, J. Salocot, F. Salman, S. Molina-Obando, P. Brooks, M. Bui, M. Lichtenberger, E. Tamboboy, K. Molloy, A. E. Santana-Cruz, A. Hernandez, S. Yu, A. Diwan, M. Patel, T. R. Aiken, S. Morejohn, S. Koskela, T. Yang, D. Lehmann, J. Chojetzki, S. Sisodiya, S. Koolman, P. K. Shiu, S. Cho, A. Bast, B. Reicher, M. Blanquart, L. Houghton, H. Choi, M. Ioannidou, M. Collie, J. Eckhardt, B. Gorko, L. Guo, Z. Zheng, A. Poh, M. Lin, I. Taisz, W. Murfin, Á. S. Díez, N. Reinhard, P. Gibb, N. Patel, S. Kumar, M. Yun, M. Wang, D. Jones, L. Encarnacion-Rivera, A. Oswald, A. Jadia, M. Erginkaya, N. Drummond, L. Walter, I. Tastekin, X. Zhong, Y. Mabuchi, F. J. F. Santiago, U. Verma, N. Byrne, E. Kunze, T. Crahan, R. Margossian, H. Kim, I. Georgiev, F. Szorenyi, A. Adachi, B. Bargeron, T. Stürner, D. Demarest, B. Gür, A. N. Becker, R. Turnbull, A. Morren, A. Sandoval, A. Moreno-Sanchez, D. A. Pacheco, E. Samara, H. Croke, A. Thomson, C. Laughland, S. B. Dutta, P. G. A. de Antón, B. Huang, P. Pujols, I. Haber, A. González-Segarra, D. T. Choe, V. Lukyanova, N. Mancini, Z. Liu, T. Okubo, M. A. Flynn, G. Vitelli, M. Laturney, F. Li, S. Cao, C. Manyari-Diaz, H. Yim, A. D. Le, K. Maier, S. Yu, Y. Nam, D. Bąba, A. Abusaif, A. Francis, J. Gayk, S. S. Huntress, R. Barajas, M. Kim, X. Cui, G. R. Sterne, A. Li, K. Park, G. Dempsey, A. Mathew, J. Kim, T. Kim, G.-t. Wu, S. Dhawan, M. Brotas, C.-h. Zhang, S. Bailey, A. Del Toro, R. Yang, S. Gerhard, A. Champion, D. J. Anderson, R. Behnia, S. S. Bidaye, A. Borst, E. Chiappe, K. J. Colodner, A. Dacks, B. Dickson, D. Garcia, S. Hampel, V. Hartenstein, B. Hassan, C. Helfrich-Forster, W. Huetteroth, J. Kim, S. S. Kim, Y.-J. Kim, J. Y. Kwon, W.-C. Lee, G. A. Linneweber, G. Maimon, R. Mann, S. Noselli, M. Pankratz, L. Prieto-Godino, J. Read, M. Reiser, K. von Reyn, C. Ribeiro, K. Scott, A. M. Seeds, M. Selcho, M. Silies, J. Simpson, S. Waddell, M. F. Wernet, R. I. Wilson, F. W. Wolf, Z. Yao, N. Yapici, M. Zandawala, FlyWire Consortium, Neuronal wiring diagram of an adult brain. *Nature* **634**, 124–138 (2024).
51. N. Eckstein, A. S. Bates, A. Champion, M. Du, Y. Yin, P. Schlegel, A. K.-Y. Lu, T. Rymer, S. Finley-May, T. Paterson, R. Parekh, S. Dorkenwald, A. Matsliah, S.-C. Yu, C. McKellar, A. Sterling, K. Eichler, M. Costa, S. Seung, M. Murthy, V. Hartenstein, G. S. X. E. Jefferis, J. Funke, Neurotransmitter classification from electron microscopy images at synaptic sites in *Drosophila melanogaster*. *Cell* **187**, 2574–2594.e23 (2024).
52. O. T. Shafer, M. Rosbash, J. W. Truman, Sequential nuclear accumulation of the clock proteins period and timeless in the pacemaker neurons of *Drosophila melanogaster*. *J. Neurosci.* **22**, 5946–5954 (2002).
53. Z. Zhu, J. Lennon, T. M. Barry, T. S. Ortiz, S. Lymer, S. Mezan, S. Kadener, J. Blau, A gene expression program activated by neuronal inactivity. bioRxiv 636878 [Preprint] (2024). https://doi.org/10.1101/636878.
54. D. G. Gundermann, S. Lymer, J. Blau, A rapid and dynamic role for FMRP in the plasticity of adult neurons. *bioRxiv*, doi.org/10.1101/2023.1109.1101.555985 , (2023).
55. S. Cachero, M. Gkantia, A. S. Bates, S. Frechter, L. Blackie, A. McCarthy, B. Sutcliffe, A. Strano, Y. Aso, G. S. X. E. Jefferis, BAcTrace, a tool for retrograde tracing of neuronal circuits in *Drosophila*. *Nat. Methods* **17**, 1254–1261 (2020).
56. E. Blanchardon, B. Grima, A. Klarsfeld, E. Chelot, P. E. Hardin, T. Preat, F. Rouyer, Defining the role of *Drosophila* lateral neurons in the control of circadian rhythms in motor activity and eclosion by targeted genetic ablation and PERIOD protein overexpression. *Eur. J. Neurosci.* **13**, 871–888 (2001).
57. F. Lehmann-Horn, K. Jurkat-Rott, Voltage-gated ion channels and hereditary disease. *Physiol. Rev.* **79**, 1317–1372 (1999).
58. M. N. Nitabach, Y. Wu, V. Sheeba, W. C. Lemon, J. Strumbos, P. K. Zelensky, B. H. White, T. C. Holmes, Electrical hyperexcitation of lateral ventral pacemaker neurons desynchronizes downstream circadian oscillators in the fly circadian circuit and induces multiple behavioral periods. *J. Neurosci.* **26**, 479–489 (2006).
59. D. Stoleru, Y. Peng, P. Nawathean, M. Rosbash, A resetting signal between *Drosophila* pacemakers synchronizes morning and evening activity. *Nature* **438**, 238–242 (2005).
60. Z. Yao, A. J. Bennett, J. L. Clem, O. T. Shafer, The *Drosophila* clock neuron network features diverse coupling modes and requires network-wide coherence for robust circadian rhythms. *Cell Rep.* **17**, 2873–2881 (2016).
61. M. S. Chen, R. A. Obar, C. C. Schroeder, T. W. Austin, C. A. Poodry, S. C. Wadsworth, R. B. Vallee, Multiple forms of dynamin are encoded by shibire, a *Drosophila* gene involved in endocytosis. *Nature* **351**, 583–586 (1991).
62. T. Kosaka, K. Ikeda, Reversible blockage of membrane retrieval and endocytosis in the garland cell of the temperature-sensitive mutant of *Drosophila melanogaster*, shibirets1. *J. Cell Biol.* **97**, 499–507 (1983).
63. C. Wegener, E. Amini, J. Cavieres-Lepe, J. Ewer, Neuronal and endocrine mechanisms underlying the circadian gating of eclosion: Insights from *Drosophila*. *Curr. Opin. Insect Sci.* **66**, 101286 (2024).
64. C. Helfrich-Forster, Development of pigment-dispersing hormone-immunoreactive neurons in the nervous system of *Drosophila melanogaster*. *J. Comp. Neurol.* **380**, 335–354 (1997).
65. S. Hidalgo, M. Anguiano, C. A. Tabuloc, J. C. Chiu, Seasonal cues act through the circadian clock and pigment-dispersing factor to control EYES ABSENT and downstream physiological changes. *Curr. Biol.* **33**, 675–687.e5 (2023).
66. K. M. Parisky, J. Agosto, S. R. Pulver, Y. Shang, E. Kuklin, J. J. Hodge, K. Kang, X. Liu, P. A. Garrity, M. Rosbash, L. C. Griffith, PDF cells are a GABA-responsive wake-promoting component of the *Drosophila* sleep circuit. *Neuron* **60**, 672–682 (2008).
67. Y. Miyasako, Y. Umezaki, K. Tomioka, Separate sets of cerebral clock neurons are responsible for light and temperature entrainment of *Drosophila* circadian locomotor rhythms. *J. Biol. Rhythms* **22**, 115–126 (2007).
68. P. J. Shaw, C. Cirelli, R. J. Greenspan, G. Tononi, Correlates of sleep and waking in *Drosophila melanogaster*. *Science* **287**, 1834–1837 (2000).
69. J. C. Hendricks, S. M. Finn, K. A. Panckeri, J. Chavkin, J. A. Williams, A. Sehgal, A. I. Pack, Rest in *Drosophila* is a sleep-like state. *Neuron* **25**, 129–138 (2000).
70. T. D. Wiggin, P. R. Goodwin, N. C. Donelson, C. Liu, K. Trinh, S. Sanyal, L. C. Griffith, Covert sleep-related biological processes are revealed by probabilistic analysis in *Drosophila*. *Proc. Natl. Acad. Sci. U.S.A.* **117**, 10024–10034 (2020).
71. B. A. Stahl, M. E. Slocumb, H. Chaitin, J. R. DiAngelo, A. C. Keene, Sleep-dependent modulation of metabolic rate in *Drosophila*. *Sleep* **40**, zxs084 (2017).
72. L. Abhilash, O. T. Shafer, A two-process model of *Drosophila* sleep reveals an inter-dependence between circadian clock speed and the rate of sleep pressure decay. *Sleep* **47**, zsad277 (2023).
73. B. van Alphen, E. R. Semenza, M. Yap, B. van Swinderen, R. Allada, A deep sleep stage in *Drosophila* with a functional role in waste clearance. *Sci. Adv.* **7**, eabc2999 (2021).
74. P. H. Taghert, O. T. Shafer, Mechanisms of clock output in the *Drosophila* circadian pacemaker system. *J. Biol. Rhythms* **21**, 445–457 (2006).
75. T. Liu, G. Mahesh, J. H. Houl, P. E. Hardin, Circadian activators are expressed days before they initiate clock function in late pacemaker neurons from *Drosophila*. *J. Neurosci.* **35**, 8662–8671 (2015).
76. M. Kaneko, C. Helfrich-Forster, J. C. Hall, Spatial and temporal expression of the period and timeless genes in the developing nervous system of *Drosophila*: Newly identified pacemaker candidates and novel features of clock gene product cycling. *J. Neurosci.* **17**, 6745–6760 (1997).
77. M. Kaneko, J. C. Hall, Neuroanatomy of cells expressing clock genes in *Drosophila*: Transgenic manipulation of the period and timeless genes to mark the perikarya of circadian pacemaker neurons and their projections. *J. Comp. Neurol.* **422**, 66–94 (2000).
78. C. Helfrich-Forster, O. T. Shafer, C. Wulbeck, E. Grieshaber, D. Rieger, P. Taghert, Development and morphology of the clock-gene-expressing lateral neurons of *Drosophila melanogaster*. *J. Comp. Neurol.* **500**, 47–70 (2007).
79. M. Selcho, B. Mühlbauer, R. Hensgen, S. Shiga, C. Wegener, K. Yasuyama, Anatomical characterization of PDF-tri neurons and peptidergic neurons associated with eclosion behavior in *Drosophila*. *J. Comp. Neurol.* **526**, 1307–1328 (2018).
80. K. Yasuyama, I. A. Meinertzhagen, Synaptic connections of PDF-immunoreactive lateral neurons projecting to the dorsal protocerebrum of *Drosophila melanogaster*. *J. Comp. Neurol.* **518**, 292–304 (2010).
81. O. T. Shafer, D. J. Kim, R. Dunbar-Yaffe, V. O. Nikolaev, M. J. Lohse, P. H. Taghert, Widespread receptivity to neuropeptide PDF throughout the neuronal circadian clock network of *Drosophila* revealed by real-time cyclic AMP imaging. *Neuron* **58**, 223–237 (2008).
82. N. Pirez, S. G. Bernabei-Cornejo, M. Fernandez-Acosta, J. M. Duhart, M. F. Ceriani, Contribution of non-circadian neurons to the temporal organization of locomotor activity. *Biol. Open* **8**, bio039628 (2018).

83. A. Ehrlich, A. A. Xu, S. Luminari, S. Kidd, C. D. Treiber, J. Russo, J. Blau, Tango-seq: Overlaying transcriptomics on connectomics to identify neurons downstream of *Drosophila* clock neurons. bioRxiv 595372 [Preprint] (2024). https://doi.org/10.1101/2024.1105.1122.595372.
84. M. P. Fernandez, J. Berni, M. F. Ceriani, Circadian remodeling of neuronal circuits involved in rhythmic behavior. *PLOS Biol.* **6**, 0518–0524 (2008).
85. A. F. Neitz, B. M. Carter, M. F. Ceriani, M. H. Ellisman, H. O. de la Iglesia, Suprachiasmatic nucleus VIPergic fibers show a circadian rhythm of expansion and retraction. *Curr. Biol.* **34**, 4056–4061.e2 (2024).
86. A. Sivachenko, Y. Li, K. C. Abruzzi, M. Rosbash, The transcription factor Mef2 links the *Drosophila* core clock to Fas2, neuronal morphology, and circadian behavior. *Neuron* **79**, 281–292 (2013).
87. M. Sekiguchi, N. Reinhard, A. Fukuda, S. Katoh, D. Rieger, C. Helfrich-Forster, T. Yoshii, A detailed re-examination of the period gene rescue experiments shows that four to six cryptochrome-positive posterior dorsal clock neurons (DN(1p)) of *Drosophila melanogaster* can control morning and evening activity. *J. Biol. Rhythms* **39**, 463–483 (2024).
88. A. Chatterjee, J. De, B. Martin, E. Chélot, F. Rouyer, Neuropeptide dynamics coordinate layered plasticity mechanisms adapting *Drosophila* circadian behavior to changing environment. bioRxiv 618497 [Preprint] (2024). https://doi.org/10.1101/2024.10.15.618497.
89. Y. Fujiwara, C. Hermann-Luibl, M. Katsura, M. Sekiguchi, T. Ida, C. Helfrich-Forster, T. Yoshii, The CCHamide1 neuropeptide expressed in the anterior dorsal neuron 1 conveys a circadian signal to the ventral lateral neurons in *Drosophila melanogaster*. *Front. Physiol.* **9**, 1276 (2018).
90. M. H. Alpert, D. D. Frank, E. Kaspi, M. Flourakis, E. E. Zaharieva, R. Allada, A. Para, M. Gallio, A circuit encoding absolute cold temperature in *Drosophila*. *Curr. Biol.* **30**, 2275–2288.e5 (2020).
91. F. Guo, J. Yu, H. J. Jung, K. C. Abruzzi, W. Luo, L. C. Griffith, M. Rosbash, Circadian neuron feedback controls the *Drosophila* sleep–activity profile. *Nature* **536**, 292–297 (2016).
92. G. W. Meissner, A. Vannan, J. Jeter, K. Close, G. M. DePasquale, Z. Dorman, K. Forster, J. A. Beringer, T. Gibney, J. H. Hausenfluck, Y. He, K. Henderson, L. Johnson, R. M. Johnston, G. Ihrke, N. A. Iyer, R. Lazarus, K. Lee, H. H. Li, H. P. Liaw, B. Melton, S. Miller, R. Motaher, A. Novak, O. Ogundeyi, A. Petruncio, J. Price, S. Protopapas, S. Tae, J. Taylor, R. Vorimo, B. Yarbrough, K. X. Zeng, C. T. Zugates, H. Dionne, C. Angstadt, K. Ashley, A. Cavallaro, T. Dang, G. A. Gonzalez III, K. L. Hibbard, C. Huang, J. C. Kao, T. Laverty, M. Mercer, B. Perez, S. R. Pitts, D. Ruiz, V. Vallanadu, G. Z. Zheng, C. Goina, H. Otsuna, K. Rokicki, R. R. Svirskas, H. S. J. Cheong, M. J. Dolan, E. Ehrhardt, K. Feng, B. E. I. Galfi, J. Goldammer, S. J. Huston, N. Hu, M. Ito, C. McKellar, R. Minegishi, S. Namiki, A. Nern, C. E. Schretter, G. R. Sterne, L. Venkatasubramanian, K. Wang, T. Wolff, M. Wu, R. George, O. Malkesman, Y. Aso, G. M. Card, B. J. Dickson, W. Korff, K. Ito, J. W. Truman, M. Zlatic, G. M. Rubin, FlyLight Project Team, A split-GAL4 driver line resource for *Drosophila* neuron types. *eLife* **13**, 98405 (2025).
93. P. Schlegel, Y. Yin, A. S. Bates, S. Dorkenwald, K. Eichler, P. Brooks, D. S. Han, M. Gkantia, M. dos Santos, E. J. Munnelly, G. Badalamente, L. S. Capdevila, V. A. Sane, A. M. C. Fragniere, L. Kiassat, M. W. Pleijzier, T. Stürner, I. F. M. Tamimi, C. R. Dunne, I. Salgarella, A. Javier, S. Fang, E. Perlman, T. Kazimiers, FlyWire Consortium, M. Costa, H. S. Seung, M. Murthy, V. Hartenstein, D. D. Bock, G. S. X. E. Jefferis, Whole-brain annotation and multi-connectome cell typing of *Drosophila*. *Nature* **634**, 139–152 (2024).
94. C. Pfeiffenberger, B. C. Lear, K. P. Keegan, R. Allada, Processing circadian data collected from the *Drosophila* activity monitoring (DAM) system. *Cold Spring Harb Protoc.* **2010**, pdb.prot5519 (2010).
95. J. L. Persons, L. Abhilash, A. J. Lopatkin, A. Roelofs, E. V. Bell, M. P. Fernandez, O. T. Shafer, PHASE: An open-source program for the analysis of *Drosophila* phase, activity, and sleep under entrainment. *J. Biol. Rhythms* **37**, 455–467 (2022).
96. J. Cavieres-Lepe, E. Amini, M. Zabel, D. R. Nassel, R. Stanewsky, C. Wegener, J. Ewer, Timed receptor tyrosine kinase signaling couples the central and a peripheral circadian clock in *Drosophila*. *Proc. Natl. Acad. Sci. U.S.A.* **121**, e2308067121 (2024).
97. J. D. Levine, P. Funes, H. B. Dowse, J. C. Hall, Signal analysis of behavioral and molecular cycles. *BMC Neurosci.* **3**, 1 (2002).
98. M. Ruben, M. D. Drapeau, D. Mizrak, J. Blau, A mechanism for circadian control of pacemaker neuron excitability. *J. Biol. Rhythms* **27**, 353–364 (2012).

Acknowledgments: We are grateful to P. Emery, J. Blau, and members of the Fernández Lab for discussions and to O. Shafer for comments on the manuscript and assistance with and access to the FV3000 microscope. We also thank the Janelia FlyLight Project Team for the help with *split-GAL4* screening and imaging, J. Blau, P. Taghert, and C. O'Kane for sharing the fly lines, and A. Lakshman for the code to obtain *P*(wake) and *P*(doze) values. Stocks obtained from the Bloomington Drosophila Stock Center (NIH P40OD018537) were used in this study. The mouse anti-PDF antibody was obtained from the Developmental Studies Hybridoma Bank, created by the NICHD of the NIH and maintained at the University of Iowa, Department of Biology, Iowa City, IA 52242. **Funding:** This work was supported by a Beckman Foundation Scholarship to E.S.-C., a Chilean National Fund for Scientific and Technological Development grant (FONDECYT #1221270) to J.E., an NSF CAREER award (IOS-2239994) to M.P.F., and an NIH (R01NS118012) grant subaward to M.P.F. **Author contributions:** E.S.-C.: Writing—original draft, conceptualization, investigation, writing—review and editing, data curation, validation, formal analysis, and visualization. A.R.I.: Conceptualization, investigation, writing—review and editing, methodology, supervision, and formal analysis. A.N.: Investigation, writing—review and editing, and resources. J.E.: Investigation, writing—review and editing, resources, funding acquisition, data curation, formal analysis, and visualization. M.P.F.: Writing—original draft, conceptualization, investigation, writing—review and editing, resources, funding acquisition, validation, supervision, formal analysis, project administration, and visualization. **Conflict of interest statement:** The authors declare that they have no competing interests. **Data and materials availability:** All data needed to evaluate the conclusions in the paper are present in the paper and/or the Supplementary Materials. The raw data for behavior experiments have been deposited on FigShare: https://figshare.com/projects/Scholz-Carlson_et_al_Raw_Data/230804.

Submitted 7 February 2025
Accepted 1 August 2025
Published 3 September 2025
10.1126/sciadv.adw4666